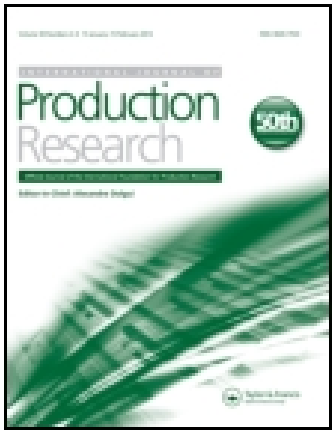

International Journal of Production Research

Publication details, including instructions for authors and subscription information:
http://www.tandfonline.com/loi/tprs20

Engineering model-based Bayesian monitoring of ramp-up phase of multistage manufacturing process

Shichang Du[ab], Xufeng Yao[c] & Delin Huang[a]

[a] Department of Industrial Engineering and Management, School of Mechanical Engineering, Shanghai Jiaotong University, Shanghai, P.R. China

[b] State Key Lab of Mechanical System and Vibration, Shanghai Jiaotong University, Shanghai, P.R. China

[c] Department of Mechanical and Industrial Engineering, University of Illinois, Chicago, IL, USA

Published online: 29 Jan 2015.

To cite this article: Shichang Du, Xufeng Yao & Delin Huang (2015) Engineering model-based Bayesian monitoring of ramp-up phase of multistage manufacturing process, International Journal of Production Research, 53:15, 4594-4613, DOI: 10.1080/00207543.2015.1005247

To link to this article: http://dx.doi.org/10.1080/00207543.2015.1005247

International Journal of Production Research, 2015
Vol. 53, No. 15, 4594–4613, http://dx.doi.org/10.1080/00207543.2015.1005247

Engineering model-based Bayesian monitoring of ramp-up phase of multistage manufacturing process

Shichang Du[a,b]*, Xufeng Yao[c] and Delin Huang[a]

[a]*Department of Industrial Engineering and Management, School of Mechanical Engineering, Shanghai Jiaotong University, Shanghai, P.R. China;* [b]*State Key Lab of Mechanical System and Vibration, Shanghai Jiaotong University, Shanghai, P.R. China;* [c]*Department of Mechanical and Industrial Engineering, University of Illinois, Chicago, IL, USA*

(*Received 18 November 2013; accepted 28 December 2014*)

Process monitoring of full mass production phase of multistage manufacturing processes (MMPs) has been successfully implemented in many applications; however, monitoring of ramp-up phase of MMPs is often more difficult to conduct due to the limited information to establish valid process control parameters (such as mean and variance). This paper focuses on the estimation of the process control parameters used for monitoring scheme design of ramp-up phase of MMPs. An engineering model of variation propagation of an MMP is developed and reconstructed to a linear model, establishing a relationship between the error sources and the variation of product characteristics. Based on the developed linear model, a two-step Bayesian method is proposed to estimate the process control parameters. The performance of the proposed Bayesian method is validated with simulation data and real-world data, and the results demonstrate that the proposed method can effectively estimate process parameters during ramp-up phase of MMP.

Keywords: Bayesian method; multistage manufacturing process; engineering model; ramp-up phase; parameter estimation

1. Introduction

1.1 *Motivation*

Most manufacturing processes (e.g. semiconductor manufacturing, automotive body assembly and valve shell machining) include more than one single stage. Usually, these processes are called multistage manufacturing processes (MMPs). MMP has a cascade property (Hawkins 1993), which means the product quality of kth stage is not only affected by the manufacturing process components at kth stage, but also related to the outputs of $(k-1)$th stage (k is the stage index). The performance of conventional statistical process control (SPC) techniques generally designated for single-stage quality monitoring and diagnosis is limited due to the cascade property. Things become even more complicated and intractable when it comes to monitoring ramp-up phase of MMP without given enough information to estimate the in-control (IC) parameters (such as process mean and variance).

Since manufacturers are facing large-scale customisation, product proliferation and shorter lead time, these challenges make shortened product life cycles inevitably become the prevailing trend. Production ramp-up, as one main part of product life cycle, is the period during which a manufacturing process makes the transition from zero to full mass production at targeted levels of cost and quality. Ramp-up is needed for each new product. In the automobile industry, ramp-up time accounts for about 10–20% of a car's life cycle, and in semiconductor or hard disc drive manufacturing industry, the ramp-up time can be even larger (Terwiesch, Bohn, and Chea 2001; Du et al. 2008). Ramp-up time reduction is a critical objective for responding to short windows of opportunity.

Several authors devoted their efforts to shorten ramp-up time. Koren, Heisel, and Jovane (1999) claimed that systematic methodologies for online part inspection and process monitoring are the key for a rapid ramp-up. Terwiesch, Bohn, and Chea (2001) presented a case study of product transfer and production ramp-up in the hard drive industry. Haller, Peikert, and Thoma (2003) presented a method to manage cycle time by closely monitoring and limiting the work in process. Carrillo and Franza (2006) presented a method for analysis of product development and production capabilities during ramp-up phase. Du et al. (2008) presented a method which can help shorten ramp-up of a new production by eliminating the bottleneck through rapid identification and isolation of system failures during ramp-up phase.

*Corresponding author. Email: lovbin@sjtu.edu.cn

In order to shorten ramp-up time, the manufacturers need to detect the process variation and identify the root cause as early as possible. Process monitoring based on control charts can tell manufacturers whether the process is out-of-control. Once the out-of-control signal is triggered, the next step is to identify the root cause. Thus, monitoring of ramp-up phase of manufacturing process is critical to figure out quality problems as early as possible and further shorten the production life cycle.

Therefore, the fundamental motivation of this study is to monitor and detect the quality problems as early as possible in MMP with limited measurement during ramp-up phase, and further shorten the production life cycle.

1.2 *Literature review*

Lots of researches about MMPs have been conducted in the past two decades. There are two major approaches in dealing with MMPs: one is to model an MMP based on an engineering knowledge and the other is to analyse an MMP using a statistical model.

A state-space model was proposed to analyse two-dimensional variation of the automobile assembly process (Jin and Shi 1999). Some researchers studied MMPs of compliant part assembly (Hu et al. 2001; Camelio, Hu, and Ceglarek 2003; Xie et al. 2007; Huang et al. 2007a, 2007b), and some researchers utilised the state-space model to represent the machining processes (Djurdjanovic and Ni 2001; Zhou, Huang, and Shi 2003; Loose, Zhou, and Ceglarek 2007; Loose et al. 2009; Abellan-Nebot et al. 2012). Du, Lv, and Xi (2011, 2012a) developed a robust approach for root causes identification in assembly and machining processes based on engineering model. Other manufacturing processes are also studied, like the stamping process (Jiang et al. 2004) and the stretch forming processes (Suri, Otto, and Boothroyd 1999). Detailed descriptions of existing research work on variation propagation modelling and applications were provided by Shi (2006) and Shi and Zhou (2009).

Researches using statistical methods focus on two main areas: monitoring and diagnosis of MMPs. Heredia-Langner, Montgomery, and Carlyle (2002) considered partial inspection strategy for all stages. Niaki and Davoodi (2008) developed a method to establish a quality control plan system for all stages. Others considered the problem of MMP inspection with other factors, such as time-varying quality (Veatch 2000) and inspection error (Shiau 2002). A survey was given by Shetwan, Vitanov, and Tjahjono (2011).

Many approaches have been developed to monitor the full mass production phase (Du, Lv, and Xi 2012b; Du, Huang, and Lv 2013; Du and Lv 2013). A thorough review about the use of SPC techniques in multistage system, including MMPs and multistage service operations was given by Tsung, Li, and Jin (2008). Hawkins (1991, 1993) developed a regression-adjusted approach to eliminate the cascade property in monitoring MMPs. The cause-selecting chart (CSC) differs with the regression-adjusted approach since it considers MMPs with the combinations of several directly linked stages. Lots of work have been done by researchers to extend the potential use of CSC (Shu, Tsung, and Kapur 2004; Shu, Tsung, and Tsui 2005). For deep discussions about CSC, please refer to the work of Asadzadeh, Aghaie, and Yang (2008).

The method of diagnosis of MMPs can be categorised into two major kinds: (i) statistical estimation-based methods and (ii) pattern matching methods. Surveys pertaining to multistage system by Tsung, Li, and Jin (2008) and Shi and Zhou (2009) covered most topics in this area.

The statistical method in MMP researches cannot fully exert the potential use of engineering knowledge about MMPs, and the results given by statistics-based method are not so transparent. Further interpretation are always needed to gain some insights about the manufacturing processes. Zou, Tsung, and Liu (2008) integrated a multivariate change-point monitoring scheme based on an engineering model. Xiang and Tsung (2008) proposed a statistical monitoring procedure based on engineering model for monitoring an MMP.

Most of the aforementioned literatures using statistical methods focus on the full mass production phase of MMPs. Under such condition, the IC parameters could be estimated through typical statistical estimation method, such as maximum likelihood estimation or minimum norm quadratic unbiased estimation. However, researches pertaining to the ramp-up phase of MMPs have not been conducted extensively and literatures about this topic are sparse. One main reason for the inadequacy of literatures concerning monitoring the ramp-up phase of MMPs is the limited measurement information. How to utilise the information to determine the IC state of a process attracts more and more attention. In the ramp-up phase, the number of samples is too small to determine the valid process control parameters. In some extreme cases, the number of samples is so small that conventional SPC techniques are not feasible at all.

The rest of this paper is organised as follows. The architecture of the proposed methodology is described in Section 2. An engineering model of variation propagation of an MMP is built, and then is reconstructed to a new linear form in Section 3. The control parameters are estimated using the proposed Bayesian method in Section 4. The process control scheme is designed for the monitoring of ramp-up phase of an MMP in Section 5. Simulation experimental

results and performance analysis are conducted in Section 6. In Section 7, a case regarding an MMP of valve shell was used to demonstrate the proposed method. Finally, some conclusions are given in Section 8.

2. Overview of the methodology

The engineering model focuses on the propagation and accumulation of variations through the MMP. One typical linear state-space model is formulated by

$$\begin{aligned} \mathbf{x}(k) &= \mathbf{A}(k)\mathbf{x}(k-1) + \mathbf{B}(k)\mathbf{u}(k) + \mathbf{v}(k) \\ \mathbf{y}(k) &= \mathbf{C}(k)\mathbf{x}(k) + \mathbf{w}(k) \end{aligned} \tag{1}$$

where k is the stage index, $\mathbf{x}(k)$ is the state vector, representing the dimensional variation of the product characteristics, $\mathbf{y}(k)$ is the corresponding measurement variation with respect to $\mathbf{x}(k)$, $\mathbf{u}(k)$ is the error source at kth stage, which usually contains two part: the tool error $\mathbf{u}_t(k)$ and the fixture error $\mathbf{u}_f(k)$, $\mathbf{A}(k)$ is the matrix representing the relocate at stage k, $\mathbf{B}(k)$ is the error transformation matrix, and $\mathbf{C}(k)$ is the observation matrix, $\mathbf{v}(k)$ and $\mathbf{w}(k)$ are the noise of the manufacturing process and the measurement, respectively.

Note that the tool error $\mathbf{u}_t(k)$ means the difference between the tool path and its nominal path. It's a comprehensive representation of the other machining factors, such as spindle thermal-induced error, cutting force-induced error and cutting tool wear error. It is the main reason for the dimensional variation of products characteristics, and hence the main monitoring objects of MMPs in this paper.

The architecture of this methodology is depicted as Figure 1, which contains three major parts. The first part is engineering analysis (S1–S2). The state-space model of variation propagation of MMP is presented (S1), and then reconstructed to a linear form under the invariant fixture error assumption (S2). The second part is the statistical inference (S3–S7). Prior information about the tool error and the datum error is put into the linear model (S3–S5). After trial production, the measurement information (S6) can be used to yield the posterior estimation of the key characteristics (S7), which contains two parts: the posterior of datum error and the posterior of tool error. Tool error is the main error introduced by kth stage and datum error is introduced by $(k-1)$th stage. Thus, the estimation of process variation introduced by kth stage is obtained. Then, the process control scheme can be established using the posterior estimation of the variation introduced at kth stage (S8).

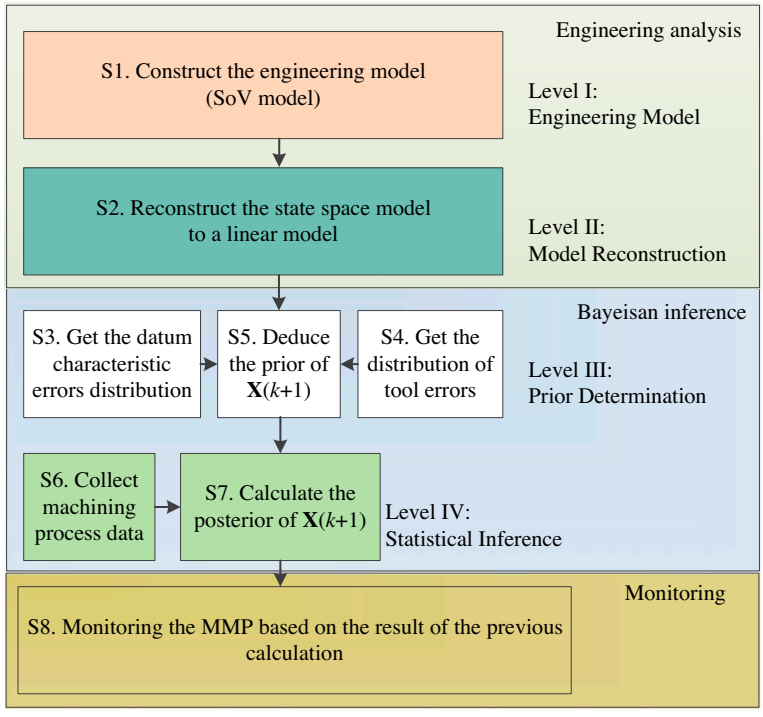

Figure 1. The architecture of the methodology.

3. The engineering model

3.1 *The state-space model*

The state-space model employs a vectorial dimensional tolerance scheme to represent the variation propagation of the product characteristics. A characteristic is represented by a coordinate system, and its variation is represented by a vector. In Figure 2(a), $O_RX_RY_RZ_R$ is the reference coordinate system (RCS) of a part and a cylindrical characteristic i on a part can be depicted using a coordinate system $O_iX_iY_iZ_i$. The relative orientation and position of every characteristic with respect to the RCS can be gotten by transforming the coordinate system corresponding to the characteristic of RCS. This transformation operation can be expressed by the homogenous transformation matrix (HTM) (see Appendix 1). In Figure 2(b), the difference between the real characteristic coordinate system (noted as A for simplicity) and its nominal coordinate system (noted as A for simplicity), is represented by a vector $(d^T, \theta^T)^T$. This vector contains two parts: a three-dimensional (3D) positional error d and a 3D angular error θ.

Analysis of the variation propagation heavily relies on four coordinate systems: machine coordinate system (MCS), RCS, fixture coordinate system (FCS) and local coordinate system (LCS, also called the characteristic coordinate system). The difference between LCS and MCS is regarded as tool error, the difference between MCS and FCS is viewed as fixture error, the difference between FCS and RCS is datum error and overall characteristic error is the difference between LCS and RCS. All of these relationships are illustrated in Figure 3.

Based on definitions of characteristics, variation and the relationships among the four coordinate systems, an MMP can be modelled using the differential motion vector and HTM. The whole computing logic of state-space model is illustrated in Figure 4.

The state-space model of MMP can be established as Equations (2) and (3). For more details, please refer to the work of Zhou, Huang, and Shi (2003) for milling process and the Appendix 2 in this paper for turning process.

$$\begin{aligned}\mathbf{x}(k) &= [\mathbf{A}_1(k) + \mathbf{A}_5(k)\mathbf{A}_4(k)\mathbf{A}_2(k)\mathbf{A}_1(k)]\mathbf{x}(k-1) + \mathbf{A}_5(k)[\mathbf{A}_4(k)\mathbf{A}_3(k) \quad \mathbf{I}_{6\times 6}]\begin{bmatrix}\mathbf{u_f}(k)\\ \mathbf{u_m}(k)\end{bmatrix} + \mathbf{v}(k)\\ &= \mathbf{A}(k)\mathbf{x}(k-1) + \mathbf{B}(k)\mathbf{u}(k) + \mathbf{v}(k)\end{aligned} \tag{2}$$

$$\mathbf{y}(k) = \mathbf{C}(k)\mathbf{x}(k) + \mathbf{w}(k) \tag{3}$$

where the values of $\mathbf{x}(k-1)$, $\mathbf{u}(k)$, $\mathbf{A}_i(k)$, $\mathbf{B}(k)$, $\mathbf{C}(k)$ are calculated using the HTM, $\mathbf{v}(k)$ and $\mathbf{w}(k)$ are the process noises and are unknown, $\mathbf{A}_1(k) \sim \mathbf{A}_4(k)$ are the transformation matrixes corresponding to the operation S1–S3, and S5 in Figure 4, $\mathbf{A}_5(k)$ is a selective matrix, its unity elements position corresponds to the characteristics generated at stage k, and the other elements are all zero.

3.2 *Reconstruction of the state-space model*

In ramp-up phase of MMP, fixture wear is always so small that its error can be neglected. Once fixture error is measured, it is imported to the state-space model, and treated as a constant. Since the operations at kth stage don't affect the characteristics generated at $(k-1)$th stages, only datum characteristics and the characteristics to be generated at kth stage are considered for simplicity. Without loss of generality, the characteristic generated at kth stage is indexed as the

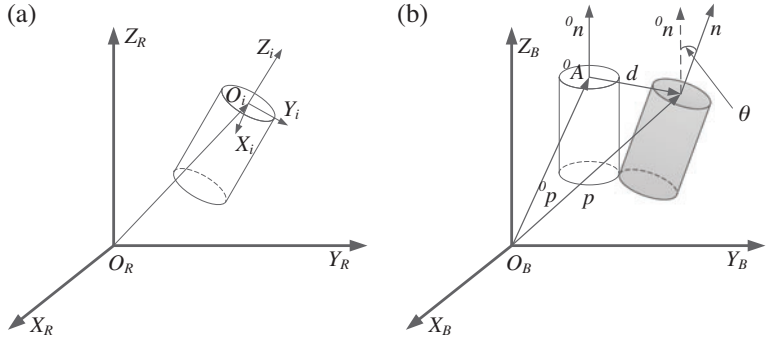

Figure 2. Characteristic and variation illustration (a) cylinder surface and (b) surface deviation representation.

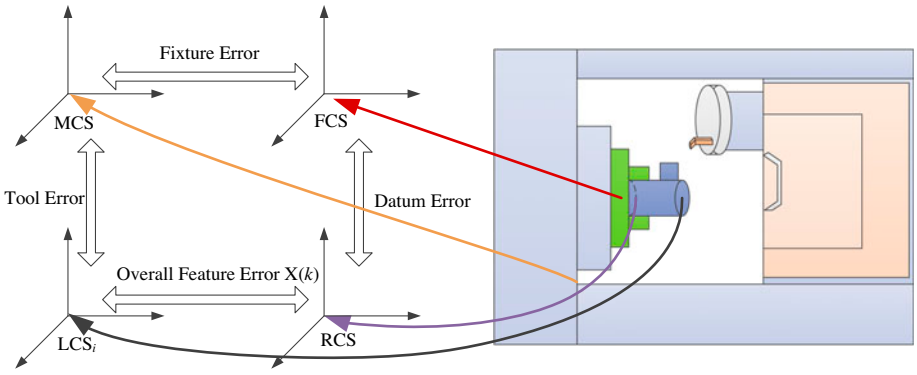

Figure 3. Relationships between coordinate systems.

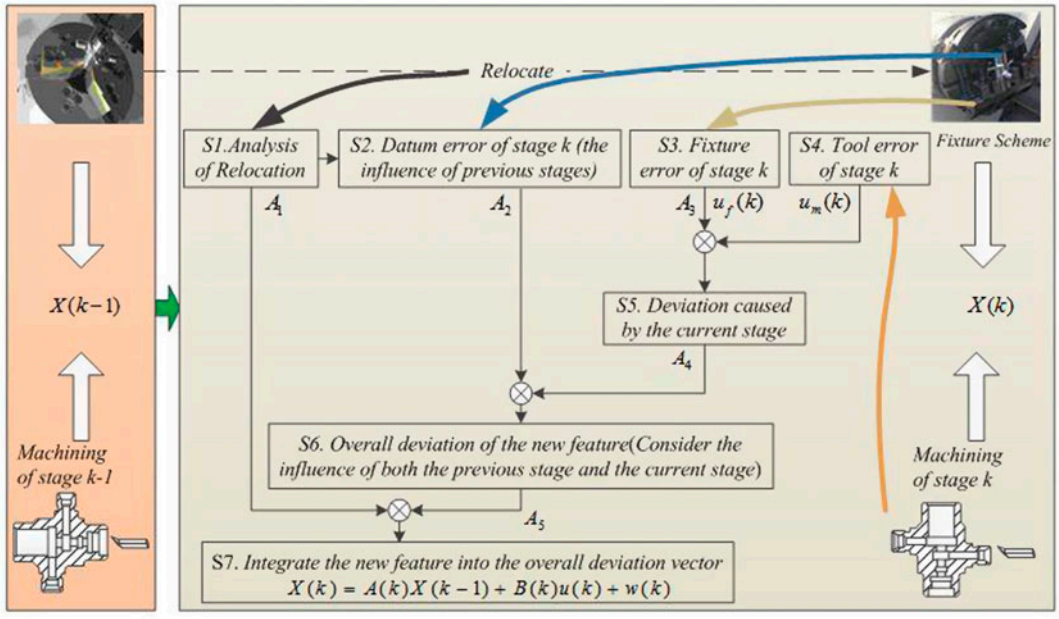

Figure 4. Computing logic of state space model.

last characteristic in the characteristic vector, and other characteristics are represented by $m-1$ positioning datum. m is the number of size parameters in product characteristic. Size parameters can be the diameter, flatness or parallelism. Thus, $\mathbf{x}(k)$ and $\mathbf{x}(k-1)$ can be represented as $6m \times 1$ vectors.

$$\mathbf{x}(k-1) = \left[\left[\left(\mathbf{x}_d^{r(k-1)}\right)^T\right]_{6(m-1)}, \mathbf{0}_6\right]^T, \mathbf{x}(k) = \left[\left[\left(\mathbf{x}_d^{r(k)}\right)^T\right]_{6(m-1)}, \left[\left(\mathbf{x}_{\text{new}}^{r(k)}\right)^T\right]_6\right]^T \tag{4}$$

where $\mathbf{x}_d^{r(k-1)}$ is the datum error with respect to the RCS at $k-1$th stage $\mathbf{x}_d^{r(k)}$ is the datum error with respect to the RCS at kth stage, and $\mathbf{x}_{\text{new}}^{r(k)}$ is the characteristic variation generated at kth stage.

For effective presentation, a new matrix extraction operation is defined. In Figure 5, $\mathbf{A}_{[\underline{a\times b}]}$ is an operation to extract the first a rows and b columns of matrix $\mathbf{A}$ and $\mathbf{A}_{[a\times\bar{b}]}$ means extracting the elements below the ath row and above the bth column of matrix $\mathbf{A}$; $\mathbf{A}_{[\underline{a}\times\bar{b}]}$ means extracting the elements of above ath rows and the elements below the bth column of matrix $\mathbf{A}$; $\mathbf{A}_{[\overline{a\times b}]}$ means extracting the elements below the ath row and the elements below the bth column of matrix $\mathbf{A}$. In the following discussion, the notation $\mathbf{A}_{a\times b}$, without any bracket, denotes the dimension of the matrix is $a \times b$.

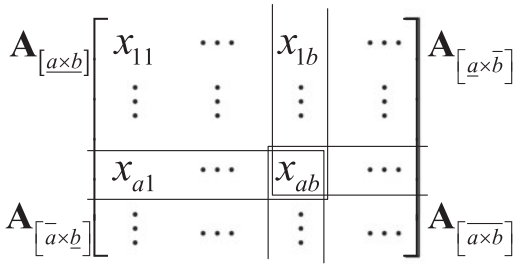

Figure 5. A new matrix extraction operation.

Using the defined matrix operation, Equation (2) can be reconstructed. Before the operation at kth stage, the variation of the key characteristic generated at kth stage is 0. Thus, Equation (2) can be expressed as:

$$\mathbf{x}(k) = [\mathbf{I}_{6m\times 6m} + \mathbf{A}_5(k)\mathbf{A}_4(k)\mathbf{A}_2(k)]\mathbf{A}_1(k)\left[\left[\left(\mathbf{x}_d^{r(k-1)}\right)^T\right]_{6(m-1)}, \mathbf{0}_6\right]^{\mathrm{T}} + \mathbf{A}_5(k)[\,\mathbf{A}_4(k)\mathbf{A}_3(k) \quad \mathbf{I}_{6\times 6}\,]\begin{bmatrix}\mathbf{u_f}(k)\\ \mathbf{u_t}(k)\end{bmatrix} \tag{5}$$

Expanding $\mathbf{A}_5(k)$, Equation (5) is converted to

$$\begin{aligned}\mathbf{x}(k) = &\left[\begin{bmatrix}\mathbf{I}_{6(m-1)\times 6(m-1)} & \mathbf{0}_{6(m-1)\times 6}\\ \mathbf{0}_{6\times 6(m-1)} & \mathbf{I}_{6\times 6}\end{bmatrix} + \begin{bmatrix}\mathbf{0}_{6(m-1)\times 6}\\ \mathbf{I}_{6\times 6}\end{bmatrix}\mathbf{A}_4(k)\mathbf{A}_2(k)\right]\mathbf{A}_1(k)\left[\left[\left(\mathbf{x}_d^{r(k-1)}\right)^T\right]_{6(m-1)}, \mathbf{0}_6\right]^{\mathrm{T}}\\ &+ \begin{bmatrix}\mathbf{0}_{6(m-1)\times 6}\\ \mathbf{I}_{6\times 6}\end{bmatrix}[\,\mathbf{A}_4(k)\mathbf{A}_3(k) \quad \mathbf{I}_{6\times 6}\,]\begin{bmatrix}\mathbf{u_f}(k)\\ \mathbf{u_t}(k)\end{bmatrix}\end{aligned} \tag{6}$$

And Equation (6) is converted into Equation (7) by performing the selective operation.

$$\mathbf{x}(k) = \begin{bmatrix}\mathbf{A}_1(k)_{\underline{[6(m-1)\times 6m]}}\\ \mathbf{A}_1(k)_{\overline{[6m-5\times 6m]}} + \mathbf{A}_4(k)\mathbf{A}_2(k)\mathbf{A}_1(k)\end{bmatrix}\left[\left[\left(\mathbf{x}_d^{r(k-1)}\right)^T\right]_{6(m-1)}, \mathbf{0}_6\right]^{\mathrm{T}} + \begin{bmatrix}\mathbf{0}_{6(m-1)\times 1}\\ [\mathbf{A}_4(k)\mathbf{A}_3(k)\mathbf{u_f}(k) + \mathbf{u_t}(k)]_{6\times 1}\end{bmatrix} \tag{7}$$

By rearranging the position of tool error and datum error, Equation (7) can be turned into

$$\mathbf{x}(k) = \begin{bmatrix}\mathbf{A}_1(k)_{\underline{[6(m-1)\times 6m]}}\\ \left[\mathbf{A}_1(k)_{\overline{[6m-5\times 6m]}} + \mathbf{A}_4(k)\mathbf{A}_2(k)\mathbf{A}_1(k)\right]_{\underline{[6\times 6(m-1)]}} \quad \mathbf{I}_{6\times 6}\end{bmatrix}\left[\left[\left(\mathbf{x}_d^{r(k-1)}\right)^T\right]_{6(m-1)}\mathbf{u_t}^T(k)\right]^{\mathrm{T}} + \begin{bmatrix}\mathbf{0}_{18\times 1}\\ [\mathbf{A}_4(k)\mathbf{A}_3(k)\mathbf{u_f}(k)]_{6\times 1}\end{bmatrix} \tag{8}$$

Combining Equation (4), Equation (8) can be converted into a linear form,

$$\left[\left[\left(\mathbf{x}_d^{r(k)}\right)^T\right]_{6(m-1)}\left[\left(\mathbf{x}_{\mathrm{new}}^{r(k)}\right)^T\right]_6\right]^{\mathrm{T}} = \Gamma(k)\left[\left[\left(\mathbf{x}_d^{r(k-1)}\right)^T\right]_{6(m-1)}\left[\mathbf{u_t}^T(k)\right]_6\right]^{\mathrm{T}} + \begin{bmatrix}\mathbf{0}_{6(m-1)}\\ [\mathbf{A}_4(k)\mathbf{A}_3(k)\mathbf{u_f}(k)]_{6\times 1}\end{bmatrix} \tag{9}$$

where $\Gamma(k) = \begin{bmatrix}\mathbf{A}_1(k)_{\underline{[6(m-1)\times 6m]}}\\ \left[\mathbf{A}_1(k)_{\overline{[6m-5\times 6m]}} + \mathbf{A}_4(k)\mathbf{A}_2(k)\mathbf{A}_1(k)\right]_{\underline{[6\times 6(m-1)]}} \quad \mathbf{I}_{6\times 6}\end{bmatrix}$ is the coefficient matrix, representing the combination of the error sources at stage k. Since $\mathbf{A}_1(k) \sim \mathbf{A}_4(k)$ are determined by fixture error, and fixture error is unchanging during the ramp-up phase. Thus, Equation (9) also represents a stable linear relationship between the variance of the characteristics generated at stage k and the error sources. This linear relationship is the basis for the statistical inference in the proposed method.

4. The proposed Bayesian method

This paper proposed a two-step Bayesian method to estimate the process control parameters (process mean and variance). The first step is to estimate the measurement posterior $\mathbf{y}^1(k)$ at stage k with the measurement data. The second step is to estimate the posterior of the variation, noted as $\mathbf{x}^1(k)$ with measurement posterior $\mathbf{y}^1(k)$.

4.1 *The prior of the machining error*

Works pertaining to the machining tool error and error compensation have been studied extensively. Ramesh, Mannan, and Poo (2000a, 2000b) gives a thorough review of machining error in view of kinematic error, geometric error and thermal induced error. A method contributed by Shin and Wei (1992) is used in this paper to elicit the prior. To shorten the length of the paper and focus on the essential content, we choose not to explain it here. For full deduction of the machine error prior, please refer to the paper by Shin and Wei (1992).

4.2 *The prior of the measurement*

The variation of the datum characteristics at the first stage could be assured by the supplier and the datum error distribution can be obtained. After the machining of stage 1, the part is transferred to stage 2, and is relocated. The datum error of stage 2 can be deduced through Equation (9). If the datum used at kth stage is produced at $(k-1)$th stage, then the variation generated at kth stage is affected by the $(k-1)$th stage's machining error through the inaccurate datum. Note that the datum of kth stage is the manufactured characteristics of $(k-1)$th stages and their distribution could be deduced from the data collected. Suppose the variation of the $(k-1)$th stage, $\mathbf{x}(k-1)$, follows a distribution $\mathbf{N}(\mu(k-1), \mathbf{\Sigma}(k-1))$. Note $\mathbf{u}_t(k)$ as the tool error, which follows a normal distribution $\mathbf{N}\big(\mu_t(k), \mathbf{\Sigma}_t(k)\big)$. The distribution of fixture error $\mathbf{u}_f(k)$ can be considered as a degenerate distribution, noted as $\mathbf{u}_f(k) \sim N(\boldsymbol{\mu}_f(k), 0)$. Since the tool error is independent of the fixture error, $\mathbf{u}(k)$ also follows a partially degenerate distribution, noted as $\mathbf{u}(k) \sim N\left(\begin{pmatrix} \boldsymbol{\mu}_t(k) \\ \boldsymbol{\mu}_f(k) \end{pmatrix}, \begin{pmatrix} \mathbf{\Sigma}_t(k) & \mathbf{0} \\ \mathbf{0} & \mathbf{0} \end{pmatrix}\right)$. Import the distribution information into Equation (9), then $\mathbf{x}(k)$ follows a distribution $N(\boldsymbol{\mu}(k), \mathbf{\Sigma}(k))$.

Denote $\rho_{\mathbf{Y}}(\mathbf{y}(k)|\mathbf{x}(k))$ as the conditional density function of $\mathbf{y}(k)$. In normal manufacturing process, the result can be obtained by Equation (9). According to Equation (3), the expected value is shown by Equation (10).

$$E(\mathbf{y}(k)|\mathbf{x}(k)) = E(\mathbf{w}(k)|\mathbf{x}(k)) + \mathbf{C}(k)\mathbf{x}(k) \tag{10}$$

Since the measurement noise $\mathbf{w}(k)$ is independent of $\mathbf{x}(k)$ and the expectation of $\mathbf{w}(k)$ is 0, the expectation of $\mathbf{y}(k)$ is shown by Equation (11). And the variance of $\mathbf{y}(k)$ is shown by Equation (12).

$$E(\mathbf{y}(k)\mathbf{x}(k)) = E(\mathbf{w}(k)) + \mathbf{C}(k)\mathbf{x}(k) = \mathbf{C}(k)\mathbf{x}(k) \tag{11}$$

$$V(\mathbf{y}(k)|\mathbf{x}(k)) = V(\mathbf{w}(k)|\mathbf{x}(k)) = V(\mathbf{w}(k)) = \mathbf{\Sigma}_{\mathbf{w}(k)} \tag{12}$$

Denote the normal density function as $N(\mathbf{x}; \boldsymbol{\mu}, \mathbf{\Sigma})$, and suppose there are three normal density functions, noted as $N(\mathbf{x}; \mu_i, \mathbf{\Sigma}_i), i = 1, 2, 3$, then the following equations hold (Anderson 2003; Petersen and Pedersen 2006).

$$N(\mathbf{x}; \boldsymbol{\mu}, \mathbf{\Sigma}) = N(\boldsymbol{\mu}; \mathbf{x}, \mathbf{\Sigma}) \tag{13}$$

$$N(\mathbf{A}\mathbf{x}; \boldsymbol{\mu}, \mathbf{\Sigma}) = \frac{1}{|\mathbf{A}|} N\Big(\mathbf{x}; \mathbf{A}^{-1}\boldsymbol{\mu}, \mathbf{A}^{-1}\mathbf{\Sigma}\big(\mathbf{A}^T\big)^{-1}\Big) \tag{14}$$

$$N(\mathbf{x}; \boldsymbol{\mu}_1, \mathbf{\Sigma}_1) N(\mathbf{x}; \boldsymbol{\mu}_2, \mathbf{\Sigma}_2) = \zeta N(\mathbf{x}; \boldsymbol{\mu}_3, \mathbf{\Sigma}_3) \tag{15}$$

where $(\mathbf{\Sigma}_3)^{-1} = (\mathbf{\Sigma}_1)^{-1} + (\mathbf{\Sigma}_2)^{-1}$, $\boldsymbol{\mu}_3 = \mathbf{\Sigma}_3\Big((\mathbf{\Sigma}_1)^{-1}\boldsymbol{\mu}_1 + (\mathbf{\Sigma}_2)^{-1}\boldsymbol{\mu}_2\Big)$ and ζ is a constant and does not depend on $\mathbf{x}$.

$$\int_{\mathbf{x}} N(\mathbf{x}; \boldsymbol{\mu}_1, \mathbf{\Sigma}_1) N(\mathbf{x}; \mathbf{y}, \mathbf{\Sigma}_2) \mathrm{d}\mathbf{x} = N(\mathbf{y}; \boldsymbol{\mu}_1, \mathbf{\Sigma}_1 + \mathbf{\Sigma}_2) \tag{16}$$

Thus, the distribution of $\mathbf{y}(k)$ can be deduced as follows.

$$\begin{aligned} \rho_{\mathbf{Y}}(\mathbf{y}(k)) &= \textstyle\int_{\mathbf{x}} \rho_{\mathbf{Y}}(\mathbf{y}(k)|\mathbf{x}(k)) \rho_{\mathbf{X}}(\mathbf{x}(k)) \mathrm{d}\mathbf{x} \\ &= \textstyle\int_{\mathbf{x}} N\Big(\mathbf{y}; \mathbf{C}(k)\mathbf{x}(k), \Sigma_{\mathbf{W}^0(k)}\Big) N\big(\mathbf{x}; \boldsymbol{\mu}^0(k), \mathbf{\Sigma}^0(k)\big) \mathrm{d}\mathbf{x} \end{aligned} \tag{17}$$

According to Equation (13), Equation (17) can be transformed as:

$$\rho_{\mathbf{Y}}(\mathbf{y}(k)) = \int_{\mathbf{x}} N\left(\mathbf{C}(k)\mathbf{x}(k); \mathbf{y}, \Sigma_{\mathbf{w}(k)}\right) N(\mathbf{x}; \boldsymbol{\mu}(k), \boldsymbol{\Sigma}(k))\mathrm{d}\mathbf{x} \tag{18}$$

According to Equation (14),

$$\rho_{\mathbf{Y}}(\mathbf{y}(k)) = \frac{1}{|\mathbf{C}(k)|}\int_{\mathbf{x}} N\left(\mathbf{x}(k); (\mathbf{C}(k))^{-1}\mathbf{y}, (\mathbf{C}(k))^{-1}\Sigma_{\mathbf{w}(k)}\left((\mathbf{C}(k))^{T}\right)^{-1}\right) N(\mathbf{x}; \boldsymbol{\mu}(k), \boldsymbol{\Sigma}(k))\mathrm{d}\mathbf{x} \tag{19}$$

Applying Equation (16), it can be written as

$$\rho_{\mathbf{Y}}(\mathbf{y}(k)) = \frac{1}{|\mathbf{C}(k)|} N\left((\mathbf{C}(k))^{-1}\mathbf{y}; \boldsymbol{\mu}(k), (\mathbf{C}(k))^{-1}\Sigma_{\mathbf{w}(k)}\left((\mathbf{C}(k))^{T}\right)^{-1} + \boldsymbol{\Sigma}(k)\right) \tag{20}$$

Using Equation (14) again, the distribution of $\mathbf{y}(k)$ is shown by Equation (21).

$$\rho_{\mathbf{Y}}(\mathbf{y}(k)) = N\left(\mathbf{y}; \mathbf{C}(k)\boldsymbol{\mu}(k), \Sigma_{\mathbf{w}(k)} + \mathbf{C}(k)\boldsymbol{\Sigma}(k)(\mathbf{C}(k))^{T}\right) \tag{21}$$

So far, the prior about the measurement is obtained. After the trial production, the posterior of the measurement could be calculated using the deduction illustrated in next subsection.

4.3 *The posterior of the measurement*

Under the normal manufacturing and measurement system, the mean of the variation follows a normal distribution, and the covariance of the measurement, noted as $\boldsymbol{\Sigma}$, follows a Wishart distribution (Mardia, Kent, and Bibby 1992; Anderson 2003). And the inverse of $\boldsymbol{\Sigma}$, noted as $\boldsymbol{\Sigma}^{-1}$, is often called precision matrix, and it follows an inverse Wishart distribution. The joint probability distribution follows a multi-normal inverse Wishart distribution, noted as MN-IWishart. The prior of the variation's measurement $\left(\boldsymbol{\mu}_y^0(k), \boldsymbol{\Sigma}_y^0(k)\right)$ conforms to a MN-IWishart distribution, as shown by Equation (22).

$$\begin{aligned} P\left(\mathbf{y}^0(k), \boldsymbol{\mu}_y^0(k), \boldsymbol{\Sigma}_y^0(k)\right) = {} & \frac{1}{(2\pi)^{p/2}\sqrt{\left|\boldsymbol{\Sigma}_y^0(k)\right|}} \times \exp\left\{-\frac{1}{2}\left(\mathbf{y}^0(k)^T - \left(\boldsymbol{\mu}_y^0(k)\right)^T\right)\left[\boldsymbol{\Sigma}_y^0(k)\right]^{-1}\left(\mathbf{y}^0(k) - \boldsymbol{\mu}_y^0(k)\right)\right\} \\ & \times \pi_1\left(\boldsymbol{\Sigma}_y^0(k)\right) \times \pi_2\left(\boldsymbol{\mu}_y^0(k)\middle|\boldsymbol{\Sigma}_y^0(k)\right) \end{aligned} \tag{22}$$

where $\pi_1\left(\boldsymbol{\Sigma}_y^0(k)\right) = \frac{|\mathbf{T}|^{\alpha/2}\left|\left[\boldsymbol{\Sigma}_y^0(k)\right]^{-1}\right|^{-(\alpha+p+1)/2}\exp\left\{-\frac{1}{2}\mathrm{tr}\left(\mathbf{T}\left[\boldsymbol{\Sigma}_y^0(k)\right]^{-1}\right)\right\}}{2^{\alpha p/2}\pi^{p(p-1)/4}\prod_{i=1}^{p}\Gamma((\alpha-i+1)/2)}$, $\pi_2\left(\boldsymbol{\mu}_y^0(k)|\boldsymbol{\Sigma}_y^0(k)\right) = \frac{t^{p/2}}{(2\pi)^{p/2}\sqrt{\left|\boldsymbol{\Sigma}_y^0(k)\right|}}$ $\times \exp\left\{-\frac{t}{2}\left(\boldsymbol{\mu}_y^0(k) - \theta\right)^T\left[\boldsymbol{\Sigma}_y^0(k)\right]^{-1}\left(\boldsymbol{\mu}_y^0(k) - \theta\right)\right\}$, and α can be interpreted as the equivalent sample size of the prior knowledge about the process, t is the adjustment of the prior variance, both α and t can be seen as the confidence of the prior knowledge and p is the degree of freedom of the precision matrix.

After trial production, the posterior distribution of $\left(\boldsymbol{\mu}_y(k), \boldsymbol{\Sigma}_y(k)\right)$ can be obtained using the Bayesian formulation. Since the MN-IWishart is a conjugate prior (Rowe 2002), the posterior of the measurement is presented as follows.

$$\begin{aligned} \pi_3\left(\boldsymbol{\mu}_y(k), \boldsymbol{\Sigma}_y(k)\middle|\mathbf{y}_1, \ldots, \mathbf{y}_n\right) &= \frac{p\left(\mathbf{y}(k), \boldsymbol{\mu}_y(k), \boldsymbol{\Sigma}_y(k)\right)}{p(\mathbf{y}(k))} = \frac{p\left(\mathbf{y}(k), \boldsymbol{\mu}_y(k), \boldsymbol{\Sigma}_y(k)\right)}{\int_{\boldsymbol{\mu}_y(k), \boldsymbol{\Sigma}_y(k)} p\left(\mathbf{y}(k), \boldsymbol{\mu}_y(k), \boldsymbol{\Sigma}_y(k)\right) d\boldsymbol{\mu}_y(k) d\boldsymbol{\Sigma}_y(k)} \\ &= \pi_3\left(\boldsymbol{\Sigma}_y(k)|\mathbf{y}_1, \ldots, \mathbf{y}_n\right)\pi_4\left(\boldsymbol{\mu}_y(k)|\boldsymbol{\Sigma}_y(k); \mathbf{y}_1, \ldots, \mathbf{y}_n\right) \end{aligned} \tag{23}$$

where $\pi_3\left(\boldsymbol{\Sigma}_y(k)|\mathbf{y}_1, \ldots, \mathbf{y}_n\right) = \frac{|\mathbf{T}_n|^{\alpha_n/2}\left|\left[\boldsymbol{\Sigma}_y(k)\right]^{-1}\right|^{-(\alpha_n+p+1)/2}\exp\left\{-\frac{1}{2}\mathrm{tr}\left(\mathbf{T}_n\left[\boldsymbol{\Sigma}_y(k)\right]^{-1}\right)\right\}}{2^{\alpha_n p/2}\pi^{p(p-1)/4}\prod_{i=1}^{p}\Gamma((\alpha_n-i+1)/2)}$, $\pi_4\left(\boldsymbol{\mu}_y(k)\middle|\boldsymbol{\Sigma}_y(k); \mathbf{y}_1, \ldots, \mathbf{y}_n\right) = \frac{t_n^{p/2}}{(2\pi)^{p/2}\sqrt{\left|\boldsymbol{\Sigma}_y(k)\right|}}$ $\exp\left\{-\frac{k_n}{2}\left(\boldsymbol{\mu}_y(k) - \theta_n\right)^T\left[\boldsymbol{\Sigma}_y(k)\right]^{-1}\left(\boldsymbol{\mu}_y(k) - \theta_n\right)\right\}$,

$\alpha_n = \alpha + n$, $t_n = t + n$, $\theta_n = \frac{n\bar{\mathbf{x}} + t\theta}{n+t}$, $\mathbf{T_n} = \mathbf{T} + \mathbf{V} + \frac{t_n(\bar{\mathbf{x}} - \theta)(\bar{x} - \theta)^T}{t+n}$, θ and $\mathbf{T}$ are the prior knowledge about measurement mean and its covariance matrix, and they can be obtained through the statistical analysis of the historical data.

$$\bar{\mathbf{x}} = \sum_{i=1}^{n} \frac{\mathbf{x_i}}{n} \sim N_p\left(\boldsymbol{\mu}, \frac{\boldsymbol{\Sigma}}{n}\right), \quad \mathbf{V} = \sum_{i}^{n} (\mathbf{x_i} - \bar{\mathbf{x}})(\mathbf{x_i} - \bar{\mathbf{x}})^T \sim W_p(n-1, \boldsymbol{\Sigma})$$

Then, the Bayesian estimation of the posterior distribution of the measurement can be represented by Equation (24).

$$\hat{\boldsymbol{\mu}}_y(k) = \boldsymbol{\theta}_n, \hat{\boldsymbol{\Sigma}}_y(k) = \frac{\mathbf{T}_n}{(\alpha_n - p - 1)} \tag{24}$$

4.4 *The posterior of the variation of* kth *stage*

After the trial production, the posterior estimation of the mean of measurement $\mathbf{y}(k)$ can be obtained by Equation (24), denoted as $\mathbf{y}^1(k)$ and $\mathbf{y}^1(k) = \hat{\boldsymbol{\mu}}_y(k)$. Then the posterior of $\mathbf{x}(k)$, denoted as $\mathbf{x}^1(k)$, can be obtained by applying the Bayesian formulation.

$$\rho_{\mathbf{X}}\big(\mathbf{x}(k)|\mathbf{y}^1(k)\big) = \frac{\rho_{\mathbf{Y}}(\mathbf{y}_k|\mathbf{x}(k))\rho_{\mathbf{X}}(\mathbf{x}(k))}{\rho_{\mathbf{Y}}(\mathbf{y}^1(k))} \tag{25}$$

Expand Equation (25),

$$\rho_{\mathbf{X}}\big(\mathbf{x}(k)|\mathbf{y}^1(k)\big) = \frac{N(\mathbf{y}^1(k); \mathbf{C}(k)\mathbf{x}(k), \Sigma_{\mathbf{W}(k)})N(\mathbf{x}(k); \boldsymbol{\mu}(k), \boldsymbol{\Sigma}(k))}{\rho_{\mathbf{Y}}(\mathbf{y}^1(k))} \tag{26}$$

According to Equation (13), Equation (26) can be written as Equation (27).

$$\rho_{\mathbf{X}}\big(\mathbf{x}(k)|\mathbf{y}^1(k)\big) = \frac{N(\mathbf{C}(k)\mathbf{x}(k); \mathbf{y}^1(k), \Sigma_{\mathbf{W}(k)})N(\mathbf{x}(k); \boldsymbol{\mu}(k), \boldsymbol{\Sigma}(k))}{\rho_{\mathbf{Y}}(\mathbf{y}^1(k))} \tag{27}$$

By applying Equation (14), Equation (27) can be converted to Equation (28).

$$\rho_{\mathbf{X}}\big(\mathbf{x}(k)|\mathbf{y}^1(k)\big) = \frac{\frac{1}{|\mathbf{C}(k)|}N\left(\mathbf{x}(k); (\mathbf{C}(k))^{-1}\mathbf{y}^1(k), (\mathbf{C}(k))^{-1}\Sigma_{\mathbf{W}(k)}\left((\mathbf{C}(k))^T\right)^{-1}\right)N(\mathbf{x}(k); \boldsymbol{\mu}(k), \boldsymbol{\Sigma}(k))}{\rho_{\mathbf{Y}}(\mathbf{y}^1(k))} \tag{28}$$

Using Equation (15), Equation (28) can be converted to Equation (29).

$$\rho_{\mathbf{X}}(\mathbf{x}(k)|\mathbf{y}^1(k)) = \frac{\zeta}{|\mathbf{C}(k)|\rho_{\mathbf{Y}}(\mathbf{y}^1(k))} \times N\left(\mathbf{x}(k); \boldsymbol{\Sigma}^1(k)\left[(\mathbf{C}(k))^T\left(\Sigma_{\mathbf{W}(k)}\right)^{-1}\mathbf{C}(k)(\mathbf{C}(k))^{-1}\mathbf{y}^1(k) + (\boldsymbol{\Sigma}(k))^{-1}\boldsymbol{\mu}(k)\right], \boldsymbol{\Sigma}^1(k)\right) \tag{29}$$

Since $\rho_{\mathbf{X}}(\mathbf{x}(k)|\mathbf{y}^1(k))$ follows a normal distribution, the coefficient $\frac{\zeta}{|\mathbf{C}(k)|\rho_{\mathbf{Y}}(\mathbf{y}^1(k))}$ in Equation (29) is 1. Then, the posterior follows a distribution depicted in Equation (30).

$$\rho_{\mathbf{X}}\big(\mathbf{x}(k)|\mathbf{y}^1(k)\big) = N\left(\mathbf{x}(k); \boldsymbol{\Sigma}^1(k)\left[(\mathbf{C}(k))^T\left(\Sigma_{\mathbf{W}(k)}\right)^{-1}\mathbf{y}^1(k) + (\boldsymbol{\Sigma}(k))^{-1}\boldsymbol{\mu}(k)\right], \boldsymbol{\Sigma}^1(k)\right) = N\big(\mathbf{x}(k); \boldsymbol{\mu}^1(k), \boldsymbol{\Sigma}^1(k)\big) \tag{30}$$

where $\boldsymbol{\mu}^1(k) = \boldsymbol{\Sigma}^1(k)\left[(\mathbf{C}(k))^T\left(\Sigma_{\mathbf{W}(k)}\right)^{-1}\mathbf{y}^1(k) + (\boldsymbol{\Sigma}(k))^{-1}\boldsymbol{\mu}(k)\right]$, and $\boldsymbol{\Sigma}^1(k) = \left((\mathbf{C}(k))^T\left(\Sigma_{\mathbf{W}(k)}\right)^{-1}\mathbf{C}(k) + (\boldsymbol{\Sigma}(k))^{-1}\right)^{-1}$.

The posterior expectation of the variation can be represented as $\mathbf{x}^1(k) = \boldsymbol{\mu}_x^1(k)$. There is a linear relationship between $\mathbf{x}(k-1)$ and $\mathbf{x}(k)$, according to Equation (9). The posterior of $\mathbf{x}(k-1)$ and $\mathbf{x}^1(k-1)$ can be obtained using the Equations (25)–(30).The posterior of the datum error and the tool error at kth stage are depicted by Equation (31).

$$\rho_{\mathbf{X}}\left(\begin{pmatrix}[\mathbf{x}^1(k-1)]_{6(m-1)} \\ \mathbf{u}_t^1(k)\end{pmatrix}\middle|\mathbf{x}^1(k)\right) = N\left(\mathbf{x}(k-1); \begin{pmatrix}\left[\boldsymbol{\mu}_x^1(k-1)\right]_{6(m-1)} \\ \boldsymbol{\mu}_t^1(k)\end{pmatrix}, \begin{pmatrix}\left[\boldsymbol{\Sigma}_x^1(k-1)\right]_{6(m-1)\times 6(m-1)} & \mathbf{0} \\ \mathbf{0} & \boldsymbol{\Sigma}_x^1(k)\end{pmatrix}\right) \tag{31}$$

where $\begin{pmatrix}\left[\boldsymbol{\mu}_x^1(k-1)\right]_{\underline{[6(m-1)]}} \\ \boldsymbol{\mu}_t^1(k-1)\end{pmatrix} = \boldsymbol{\Sigma}_x^1(k-1)\left[(\Gamma(k))^T\left(\boldsymbol{\Sigma}_x^1(k)\right)^{-1}\mathbf{x}^1(k) + \left(\boldsymbol{\Sigma}^0(k-1)\right)^{-1}\begin{pmatrix}\left[\boldsymbol{\mu}_x^1(k-1)\right]_{\underline{[6(m-1)]}} \\ \boldsymbol{\mu}_t^0(k-1)\end{pmatrix}\right]$, and

$\begin{pmatrix}\left[\boldsymbol{\Sigma}_x^1(k-1)\right]_{\underline{[6(m-1)\times 6(m-1)]}} & \mathbf{0} \\ \mathbf{0} & \boldsymbol{\Sigma}_t^1(k)\end{pmatrix} = \left(\Gamma^T(k)\left(\boldsymbol{\Sigma}_x^1(k)\right)^{-1}\Gamma(k) + \begin{pmatrix}\left[\boldsymbol{\Sigma}_x^0(k-1)\right]_{\underline{[6(m-1)\times 6(m-1)]}} & \mathbf{0} \\ \mathbf{0} & \boldsymbol{\Sigma}_t^0(k)\end{pmatrix}^{-1}\right)^{-1}$.

Since tool error is the major error source for variation of product characteristic introduced at kth stage, the monitoring of kth stage can be conducted based on the Bayesian estimation by Equation (31).

5. Design of monitoring scheme

Through the Bayesian estimation, the posterior parameters of the tool error and the datum error can be drawn by Equation (31). And these parameters can be used for the design of the control limits to monitoring an MMP. This paper adopts a CSC control chart to eliminate the cascade property of MMP. According to the basic principle of CSC, the variables need to be adjusted to the cause selecting value $z(k)$. $z(k)$ is also called the residual. According to Asadzadeh, Aghaie, and Yang (2008),

$$z(k) = X(k) - \hat{X}(k) \tag{32}$$

The true variation caused by kth stage, namely $X(k)$, is substituted by the posterior $\hat{X}(k)$ (after the machining of kth stage) and the expected variation at kth stage $\hat{X}(k)$is estimated by the variation caused by$(k-1)$th stage $\mathbf{A}(k)\mathbf{X}(k-1)$ (before the machining of kth stage), the process control parameter represented by Equation (32) is adjusted as:

$$\mathbf{z}(k) = \left[\hat{\mathbf{X}}(k)_{|\mathbf{Y}(k)} - \mathbf{A}(k)\hat{\mathbf{X}}(k-1)_{|\mathbf{Y}(k-1)}\right]_{\overline{[6m-5]}} \tag{33}$$

Since the characteristic machined at kth stage is indexed as the last element of the state vector, i.e. the variation vector, the corresponding subscript of the newly machined characteristic is $\overline{[6m-5]}$. $\hat{\mathbf{X}}(k)$ and $\hat{\mathbf{X}}(k-1)$ are the estimated true variations of the part itself at kth and $(k-1)$th stages instead of the measurements. They can be obtained through Equation (31). One straightforward explanation of Equation (33) is that the statistic measures the variation caused by the current kth stage, instead of the measurements of the newly machined characteristic. More specifically, $\hat{\mathbf{X}}(k)_{|\mathbf{Y}(k)}$ represents the variation state vector of the characteristics, and the second part of Equation (33), $\mathbf{A}(k)\hat{\mathbf{X}}(k-1)_{|\mathbf{Y}(k-1)}$. is the effect of the cascade property caused by previous stages. The variation of the part at kth stage is a comprehensive metric of the errors introduced by previous stages and the errors incurred by kth stage because of the cascade property. Monitoring $\mathbf{z}(k)$, the statistic that depicts the variation caused by kth stage, is more effective than monitoring the process solely based on the direct measurement of the characteristics. Meanwhile, the variation introduced by kth stage, namely the tool errors, $\mathbf{u}_t(k)$, can be acquired according to Equation (31). In our case, $\mathbf{z}(k)$ and $\mathbf{u}_t(k)$ measure the same thing, i.e. the variation caused by kth stage. Since the distribution information of $\mathbf{u}_t(k)$ is easy to get we use it to estimate the control limits for the charting statistic $\mathbf{z}(k)$. Since $\mathbf{u}_t(k)$ follows a multi-normal distribution $N\left(\boldsymbol{\mu}_t^1(k), \boldsymbol{\Sigma}_t^1(k)\right)$, the control limits for the monitoring variable are $\mathbf{u}_t^1(k-1) \pm 3\boldsymbol{\Sigma}_t^1(k)$ for the statistic $\mathbf{z}(k)$.

Moreover, chart allocation strategy for multistage processes is one of important research topics. We aim at finding the stage in which the critical fault can be detected most quickly according to the criterion of non-centrality parameters and its corresponding average time to signal (ATS). The ATL criterion is a widely used performance measure in both industry and research (He and Grigoryan 2005; Shamsuzzaman, Lam, and Wu 2005; Zhang and Wu 2006). A smaller value of ATS denoted a quicker response to the fault. Since how to allocate a control chart for multistage processes is not the focus of this paper, a control chart allocation strategy is not discussed here. For more details, please refer to the work of Jin and Tsung (2009).

6. Simulation and results analysis

A simulation study is provided based on a real-world case of a three-step manufacturing process. For detailed information about the dimension of the rotary part and its manufacturing process, please refer to Appendix 3.

6.1 *Data generation and processing*

A simulation procedure is implemented to compare the performance of the proposed method and the traditional $\bar{X}$ control chart.

Step 1 Engineering model construction: employ the procedure described in Figure 4.

Step 2 Tool error and fixture error generation: generate randomly the tool error and fixture error which are assumed to follow a multi-normal distribution $MN(\mathbf{u}, \mathbf{0}, diag(0.01))$.

Step 3 Prior estimation: compute the mean and covariance of the features using Equations (10)–(21).
Step 4 Sample information generation: generate tool errors and input into the engineering model constructed in Step 1 for M times.
Step 5 Posterior calculation: for each of the M times, compute the posterior using Equations (22)–(31) based on Step 3 and Step 4.
Step 6 Control limits calculation: apply Equations (32) and (33) with the information provided by Step 5.
Step 7 Dimensional variation generation: generate dimensional variation with tool error expectation, $\mu_t = \mu_0 + k\sigma_0$;where $k = 0, 0.5, 1.0, 1.5, 2.0, 2.5, 3.0$, according to the stream of variation theory (Shi 2006).
Step 8 Trial run: for each k, repeat Step 7 for $R(k, i)$ times until the dimensional variation is out-of-control, where $R(k, i)$ is the number of samples it takes for the proposed monitoring method to detect an out of control signal in the ith run.
Step 9 Data collection: repeat Step 7 – Step 8 for N times, and record $R(k, i)$ for each i and k.
Step 10 ARL_1 calculation: compute the ARL_1 for each k, $ARL_1(k) = \frac{\sum_{i=1}^{N} R(k,i)}{N}$.
Step 1 – Step 3 are viewed as the prior knowledge acquisition, Step 4 – Step 5 are the ramp-up phase data generation, Step 6 is the monitoring plan set-up and Step 7 – Step 10 are the monitoring of the manufacturing process. For the control group ($\bar{X}$ control chart), the prior and posterior steps (Step 1–Step 3, and Step 5) are eliminated, and only ramp-up and the trial run (Step 4, Step 6–Step 10) are reserved for comparison.

6.2 *Results and discussion*

In the comparison between the proposed Bayesian method and the $\bar{X}$ control chart, two indexes, average run length (ARL) and estimation accuracy, are used to illustrate the differences. Estimation accuracy, in this study, is the defined as the percentage of the Bayesian estimate approaching to the real value with less discrepancy in the simulated ramp-up stage.

6.2.1 *Comparison of ARL*

An ARL study is conducted to illustrate the performance of the proposed method to detect drifts in the mean value of the dimensional variation in the y direction of the rotary part's excircle. By repeating the simulation for 10,000 times ($i = 1, 2, \ldots, 10{,}000$), the simulation result shows that the proposed method has a shorter ARL_1(out-of-control ARL) compared with the Shewhart method.

According to the simulation results table (Table 1), we can see that the ARL_0s (IC ARL) of the proposed method are close to the ARL_0 of the control group, namely the $\bar{X}$ control chart, which has a mean of 0 and control limits of ±3. However, the proposed method has a shorter ARL_1 than the matched Shewhart group. With the increase in sample size, the ARL_0 of the proposed method approaches to the ARL_0 of the control group.

The ARL_1 of the proposed method (column B in Table 1) is shorter than the traditional method (column T) when the number of samples M taken at the ramp-up phase. Shorter ARL_1 suggests the greater power to detect an out-of-control signal than the traditional method. Outperformance of the proposed method can be ascribed to the Bayesian method based on the engineering model which combines the engineering knowledge with the statistical theory, while the

Table 1. ARL_1 comparison between the proposed method and the traditional statistical method.

	M									
	10		20		30		40		50	
k	B	T	B	T	B	T	B	T	B	T
0.0	398.15	439.65	389.86	406.18	381.32	392.59	376.15	380.66	371.75	373.43
0.5	62.77	160.29	46.82	58.45	21.47	32.77	22.33	25.9	20.11	23.67
1.0	6.38	11.49	6.73	7.02	3.93	3.68	3.42	3.64	3.30	3.59
1.5	1.82	2.31	1.66	2.02	1.44	1.44	1.48	1.49	1.38	1.47
2.0	1.14	1.23	1.13	1.13	1.04	1.05	1.03	1.05	1.03	1.05
2.5	1.01	1.02	1.02	1	1.01	1	1.01	1.01	1	1
3.0	1	1	1	1	1	1	1	1	1	1

Note: B stands for the proposed Bayesian method; T stands for the traditional Shewhart method.

traditional method is only based on the statistics. The engineering part of the proposed method facilitates a statistical comparison using the direct information about the dimensional errors, while the traditional method is based on the measurement of the characteristic. Measurement, on the other hand, introduces some random noise as suggested in Equation (1), and thus lowers its efficiency. On the other hand, the statistical part of the proposed method, utilised on the prior information, which is so valuable when data source are so limited in ramp-up phase. However, these data are ignored by the traditional method, which merely relies on the information collected through the samples.

Other facts may impact the performance of the proposed method, such as the limited samples during the ramp-up phase, the wear of the tool and fixture, the omission of the second order small quantity of the engineering model, etc. To improve the proposed method in the future research, these facts may be studied.

When more samples are collected during the ramp-up phase, the ARL_1 value of the Bayesian method is closer to the value of the control group. And as suggested in Table 1, with the increase in the samples M, the difference between the proposed method and the traditional method narrows down. However, the samples we could collect in ramp-up phase is usually small, so the proposed method targeted for ramp-up phase monitoring is more powerful under such condition.

6.2.2 *Comparison of estimation accuracy and number of pre-control samples*

Two charting statistics i.e. the posterior estimation of variation $\mathbf{z}(k)$ in Equation (33) and the dimensional difference $\Delta y(k)$ are compared here to show which method provides a better estimation of the dimensional variation of the excircle in y-direction (please refer to Figure A.3) at kth stage. Here the dimensional difference $\Delta y(k)$ means the difference between direct measurement and the designed value. It is one commonly used control variable in practice. Designed information can be referred to Figure A.3. The proposed method yields a much higher accuracy provided by the same number of samples in the ramp-up phase. The estimation of the dimensional error of the excircle in the y direction (please refer to Figure A.3) provided by the proposed method is more accurate than the traditional statistical method (see Figure 6). By repeating the simulation for 10,000 times ($i = 1, 2, \ldots, 10{,}000$), the result shows that the proposed method has more accurate mean value than the traditional statistical method with a proportion about 96%, and provides a more accurate variance value for each dimensional error with a proportion about 93% in our study. In other words, the statistic used in the proposed method can provide a better estimation of the characteristic variation of part.

Because the proposed method incorporates the prior information into the calculation as if some virtual samples are collected. It buffers the influence of the unstable samples information collected in ramp-up phase, and yields more stationary estimation of the process mean and variance (see Figure 6), the control limits can be gotten with less time comparing with the traditional statistical method. The control limits is established at sample seven for the proposed method, while the traditional procedure yields the control limits at sample 34, according to one of the mostly used rules (Mackertich 1990). It can be seen that the proposed method could yield a control limit with less time and higher accuracy comparing with the traditional method, and thus shorten the ramp-up phase.

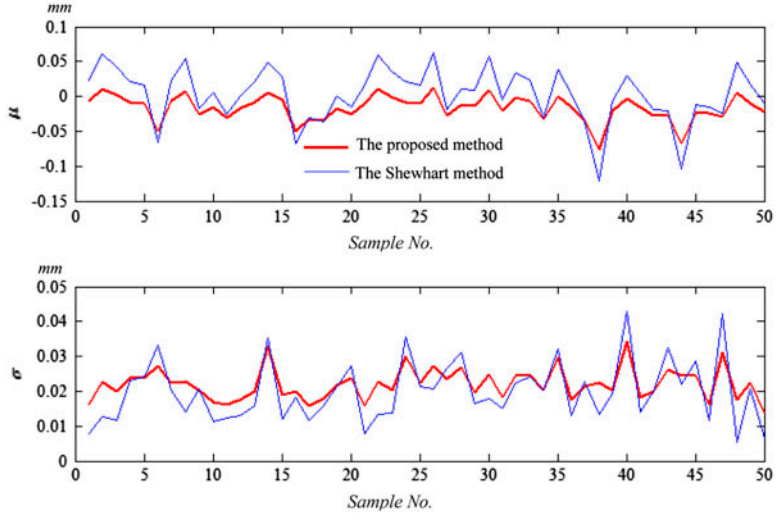

Figure 6. Comparison between the proposed method and Shewhart method.

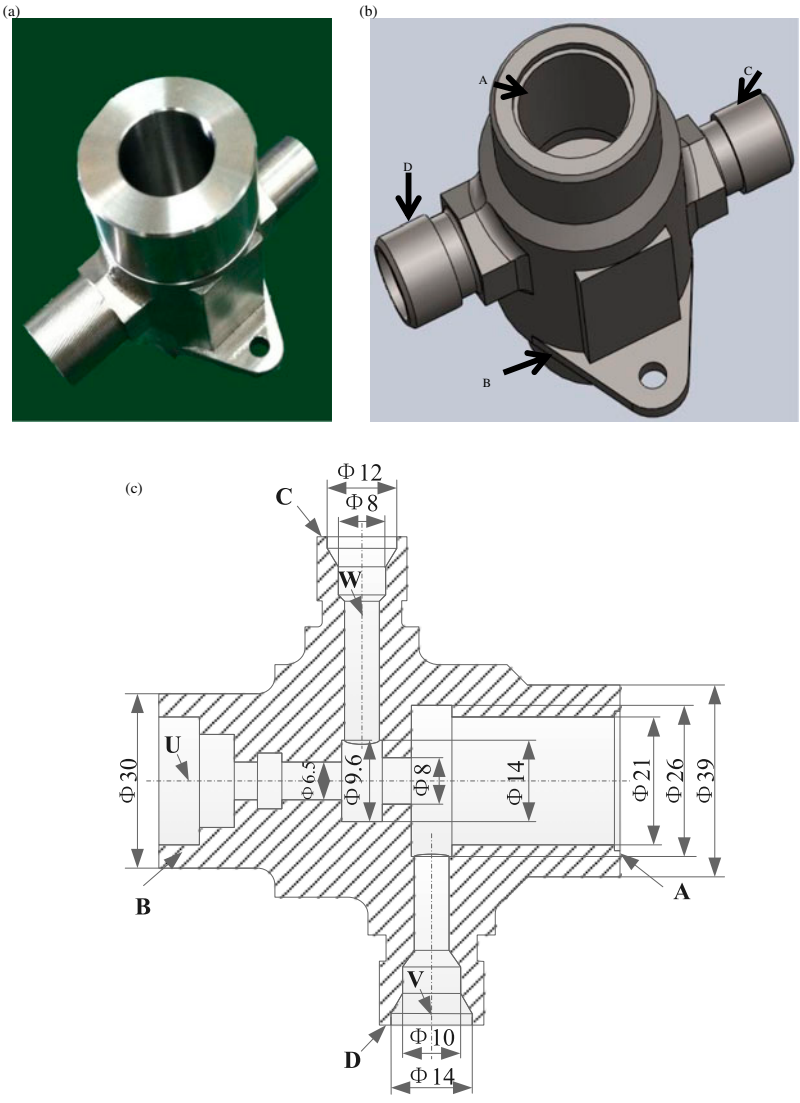

Figure 7. Valve shell.

7. Case study

7.1 *Experimental setup*

A case of MMP of valve shell is studied to validate the proposed method. Figure 7(a) depicts a raw valve shell, Figure 7(b) is a 3D model of the final product and Figure 7(c) is a cross-section drawn of valve shell from the axes of side A\B\C\D. Some positional tolerance requirement of Figure 7(c) is given by Table 2. Most of its key product characteristics are machined by turning process. As depicted by Figure 8, the whole machining process is roughly composed of five operations, noted OP10–OP50.

7.2 *Results and discussion*

The model is programmed using MATLAB 2010® based on the information of Table 2 and the 3D model in Figure 7. For *k*th stage, the variation of the product characteristics and the tool error can be output automatically once the variations of the fixture and the measurements are loaded to the programme. Once the fixture error and the estimated tool error are input, this programme can predict the variation of product characteristics at the next stage.

Table 2. Nominal positions and orientations of key product characteristics.

No.	Fixture scheme	Key product characteristics	Designed tolerances	Nominal position t_n^R/mm	Nominal angular ω_n^R/rad
OP10	B, 4-jaws Chuck	Hole Φ21	Coaxiality 0.1|axel U|	[0, 0, −29]	[0, 0, 0]
		Excircle Φ39	Not a KPC	[0, 0, 0]	[0, 0, 0]
OP20	B downward, modular fixture (process end D)	Hole Φ14	Cylindricity 0.02|V|	[−42, 0, −32.5]	[π/2, 0, π/2]
		Hole Φ10	Cylindricity 0.02|V|	[−32, 0, −32.5]	[π/2, 0, π/2]
OP30	B downward, modular fixture (process end C)	Hole Φ12	Cylindricity 0.02|W|	[−42, 0, −44.5]	[−π/2, 0, −π/2]
		Hole Φ8	Cylindricity 0.02|W|	[−32, 0, −32.5]	[−π/2, 0, −π/2]
OP40	A, 4-jaws Chuck	Slot Φ9.6	Coaxiality 0.05|U|	[0, 0, −66.5]	[0, π, 0]
		Hole Φ6.5	Coaxiality 0.05|U|	[0, 0, −62.5]	[0, π, 0]
		Excircle Φ30	Not a KPC	[0, 0, −79.5]	[0, π, 0]
OP50	B, 4-jaws Chuck	Slot Φ26	Depth 36 ± 0.1|A|	[0, 0, −36]	[0, 0, 0]
		Slot Φ14	Depth 48 ± 0.1|A|	[0, 0, −48]	[0, 0, 0]
		Hole Φ8	Coaxiality 0.05|U|	[0, 0, −35.5]	[0, 0, 0]

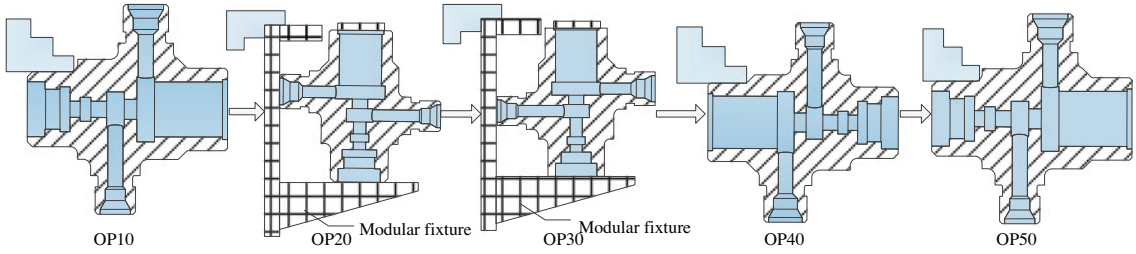

Figure 8. The MMP of valve shell.

In the machining of valve shell, the excircle of side A is manufactured at OP10 and the machined excircle A is the datum for OP40. Thus, the variation of the excircle of side A affects the characteristic of the manufacturing part at OP40. Denote $\mathbf{x}(4)$ as the total variation at OP40 after machining and $\mathbf{x}(3)$ as the total variation at OP30 after machining. By taking the characteristics involved in OP40, the dimension of the variation vector is 24×1, that is, only four characteristics are considered: three characteristics machined at OP10 and the characteristics, Φ9.6, to be machined at OP40.

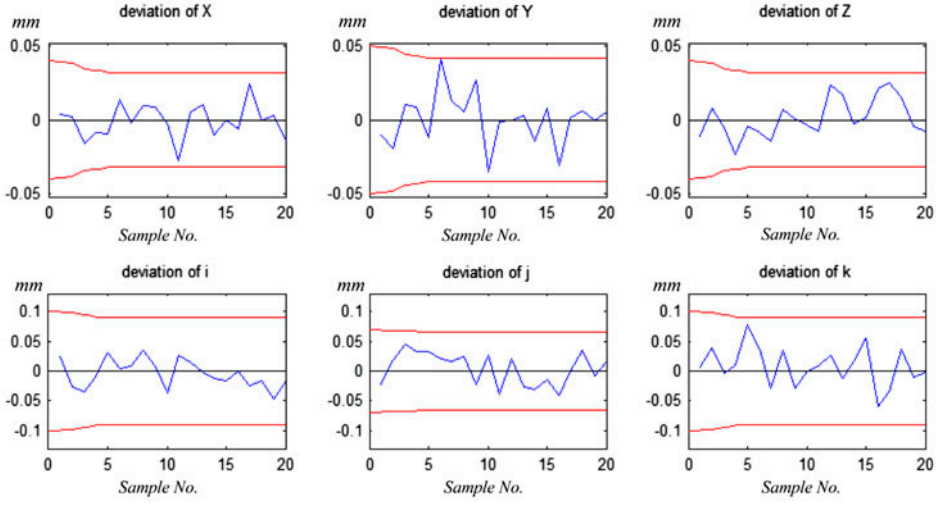

Figure 9. The control charts for coaxiality of slot Φ9.6.

$$\mathbf{x}(3) = \left[\left(\mathbf{x}_1^{r(3)}\right)^T, \left(\mathbf{x}_2^{r(3)}\right)^T, \left(\mathbf{x}_3^{r(3)}\right)^T 0\right]^{\mathrm{T}}, \mathbf{x}(4) = \left[\left(\mathbf{x}_1^{r(4)}\right)^T \left(\mathbf{x}_2^{r(4)}\right)^T \left(\mathbf{x}_3^{r(4)}\right)^T \left(\mathbf{x}_4^{r(4)}\right)^T\right]^{\mathrm{T}}.$$

The variation input of OP40 is $\left[\mathbf{u_f}(4)^T \mathbf{u_m}(4)^T\right]^T$. Since the fixture error is invariant, the only uncertain variation input is the tool error, $\mathbf{u_m}(4)^T$. According to Equation (9), the relationship between $\mathbf{x}(3)$, $\mathbf{u_m}(4)^T$ and $\mathbf{x}(4)$can be represented by Equation (34).

$$\mathbf{x}(4) = \begin{bmatrix} \mathbf{A}_1(k)_{[\underline{18\times 24}]} \\ \left[\mathbf{A}_1(k)_{[\overline{19}\times\underline{24}]} + \mathbf{A}_4(k)\mathbf{A}_2(k)\mathbf{A}_1(k)\right]_{[\underline{6\times 18}]} \end{bmatrix} \quad \mathbf{I}_{6\times 6} \left[\left[\mathbf{x}(3)\right]_{\underline{18\times 1}}^T \mathbf{u}_m^T(4)\right]^{\mathrm{T}} + \begin{bmatrix} \mathbf{0}_{18\times 1} \\ \left[\mathbf{A}_4(4)\mathbf{A}_3(4)\mathbf{u_f}(4)\right]_{6\times 1} \end{bmatrix} \tag{34}$$

According to the historical data at OP40, the distribution of the slot cutter follows a normal distribution: $\mathbf{u}_t^0(4) \sim N\left(\boldsymbol{\mu}_t^0(4), \boldsymbol{\Sigma}_t^0(4)\right)$. Then the prior distribution is gotten through Equations (10)–(17), noted as $\mathbf{x}^0(4) \sim N\left(\boldsymbol{\mu}_x^0(4), \boldsymbol{\Sigma}_x^0(4)\right)$, and $\mathbf{y}^0(4) \sim N\left(\boldsymbol{\mu}_y^0(4), \boldsymbol{\Sigma}_y^0(4)\right)$. After the trial production, some parts are manufactured through the MMP. Denote the measurement in OP40 as $\mathbf{y}_1(4), \ldots, \mathbf{y}_n(4)$. Then the posterior of the measurement can be obtained: $\mathbf{y}^1(4) \sim N\left(\boldsymbol{\mu}_y^1(4), \boldsymbol{\Sigma}_y^1(4)\right)$, and the posterior of the part characteristic Φ9.6 is $\mathbf{x}^1(4) \sim N\left(\boldsymbol{\mu}_x^1(4), \boldsymbol{\Sigma}_x^1(4)\right)$. This procedure is performed through the whole MMP. The posterior about the variation at OP40 is denoted as $N\left(\boldsymbol{\mu}_t^1(4), \boldsymbol{\Sigma}_t^1(4)\right)$. Then, the control limit is 3 $\boldsymbol{\mu}_t^1(4) \pm 3\boldsymbol{\Sigma}_t^1(4)$ for the coaxiality at OP40. Through the proposed model, the samples needed to establish control limits are reduced dramatically. This helps the MMP enter the normal production stage with less time.

The control chart can be a Shewart chart or a Hotelling T^2 chart or some more complicated charts. In this case, a group charting scheme is chosen for the independency between the six degrees of freedoms. The group charting scheme

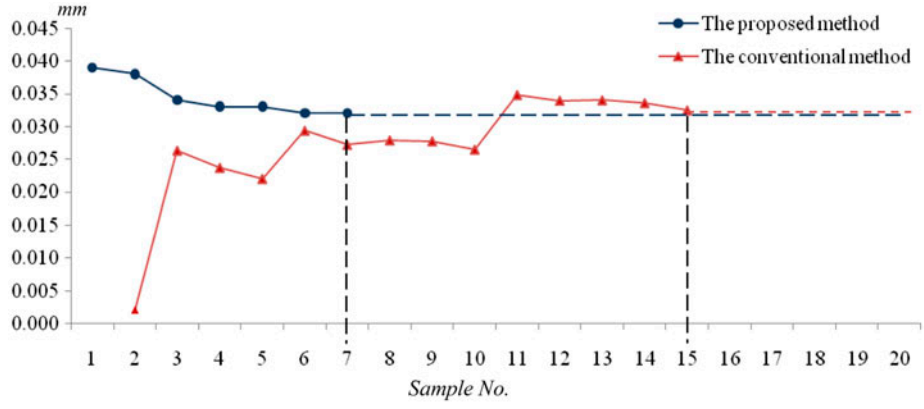

Figure 10. The upper control limits for the positional deviation in X direction.

Table 3. Estimation of dimensional error at OP50 (Unit: mm, rad).

Feature No.	1	2	3	4	5	6
X	−0.064	−0.053	0.038	0.005	0.032	0.033
Y	−0.035	−0.035	0.081	0.056	−0.043	−0.039
Z	0.021	−0.077	−0.025	−0.025	0.146	0.145
α	0.003	0.004	−0.004	−0.003	0.004	0.004
β	0.008	0.009	0.003	0.002	−0.001	0.000
γ	0.004	0.005	−0.002	−0.001	−0.004	−0.004
Feature No.	7	8	9	10	11	12
x	−0.041	−0.044	−0.046	0.043	0.062	0.075
y	−0.063	−0.065	0.070	0.059	0.063	0.061
z	0.040	0.041	0.039	0.021	0.021	0.023
α	0.005	0.006	0.005	0.004	0.004	0.006
β	−0.003	0.001	0.001	−0.006	−0.006	−0.007
γ	−0.004	−0.004	−0.002	0.025	0.025	0.026

Table 4. Partial covariance matrix (with row and column index).

	Row index							
Column index	3	38	39	44	50	56	62	68
3	0.023	−0.023	0	−0.023	−0.023	0	0	0
38	−0.023	0.045	0	0.023	0.023	0	0	0
39	0	0	0.023	0	0	−0.023	−0.023	−0.023
44	−0.023	0.023	0	0.045	0.023	0	0	0
50	−0.023	0.023	0	0.023	0.045	0	0	0
56	0	0	−0.023	0	0	0.45	0.023	0.023
62	0	0	−0.023	0	0	0.023	0.045	0.023
68	0	0	−0.023	0	0	0.023	0.023	0.045

Note: The covariance also contains a diagonal matrix consists of element 0.023.

for the coaxiality of Φ9.6 is shown as Figure 9. They are control charts for positional deviation in *X*-, *Y*- and *Z*-axis direction and angular deviation in *i*, *j* and *k*, respectively. Figure 10 is enlarged from the first subchart in Figure 9. From Figure 10, the process control parameters converges after five samples, the control limits for the positional deviation are ±0.042 mm and the control limits for the rotational deviation are ±0.09°. The proposed method reaches a steady upper control limit at the 7th sample; however, the conventional method simply uses the sample variance to set up the control limits and reaches a steady upper control limit at the 15th sample. It is much slower than the proposed method. The rule to determine the control limits is suggested by (Mackertich 1990).The numerical values of the estimation of dimensional error at OP50 and partial covariance matrix are provided in Tables 3 and 4. Since the dimension of the covariance matrix is too large, one partial matrix containing the positional error at each stage is represented. This matrix consists of a diagonal matrix with each diagonal element equals to 0.023 and other values are listed in Table 3.

8. Conclusion

This paper proposes an engineering model-based Bayesian method to estimate the process parameters in the ramp-up phase of an MMP. The state-space model is presented and reconstructed into a linear form, which represents the relationship between the error sources and the variation of the product characteristics. Based on the linear relationship, a two-step Bayesian method is formulated to estimate the process control parameters. Then, these parameters are used to establish the control limits of the CSC chart to monitoring the ramp-up phase of an MMP.

Since the proposed Bayesian method combines the engineering model with historical data, it can reduce the samples needed to estimate the process control parameters, which is very useful to the ramp-up phase monitoring of an MMP, when scarce measurement information is presented. The results of simulation experiments and case study demonstrate the effectiveness of the proposed method. The proposed method is also extensible. It can be used in-process design and evaluation (such as process capacity allocation and evaluation) and fault diagnosis (such as error pattern matching and root cause diagnosis).

Acknowledgements

The authors greatly acknowledge the editor and the referees for their valuable comments and suggestions that have led to a substantial improvement of the paper. This work was supported by the National Natural Science Foundation of China [grant number 51275558]; National Key Science and Technology Research Program of China [grant number 2014ZX04015-021]; Shanghai Rising-Star Program [grant number 13QA1402100].

Funding

This work was supported by the National Natural Science Foundation of China [grant number 51275558]; National Key Science and Technology Research Program of China [grant number 2014ZX04015-021]; Shanghai Rising-Star Program [grant number 13QA1402100].

References

Abellan-Nebot, J. V., J. Liu, F. R. Subirón, and J. Shi. 2012. "State Space Modeling of Variation Propagation in Multistation Machining Processes Considering Machining-Induced Variations." *Journal of Manufacturing Science and Engineering* 134 (2): 021002.

Anderson, T. 2003. *An Introduction to Multivariate Statistical Analysis*. 3rd ed. New York: Wiley.
Asadzadeh, S., A. Aghaie, and S. F. Yang. 2008. "Monitoring and Diagnosing Multistage Processes: A Review of Cause Selecting Control Charts." *Journal of Industrial and Systems Engineering* 2 (3): 215–236.
Cai, W., S. J. Hu, and J. Yuan. 1997. "A Variational Method of Robust Fixture Configuration Design for 3-D Workpieces." *Journal of Manufacturing Science and Engineering* 119 (4): 593–602.
Camelio, J., S. J. Hu, and D. Ceglarek. 2003. "Modeling Variation Propagation of Multi-Station Assembly Systems with Compliant Parts." *Journal of Mechanical Design* 125 (4): 673–681.
Carrillo, J. E., and R. M. Franza. 2006. "Investing in Product Development and Production Capabilities: The Crucial Linkage Between Time-to-market and Ramp-up Time." *European Journal of Operational Research* 171: 536–556.
Djurdjanovic, D., and J. Ni. 2001. "Linear State Space Modeling of Dimensional Machining Errors." *Transactions-North American Manufacturing Research Institution of SME* 29: 541–548.
Du, S., and J. Lv. 2013. "Minimal Euclidean Distance Chart Based on Support Vector Regression for Monitoring Mean Shifts of Auto-correlated Processes." *International Journal of Production Economics* 141: 377–387.
Du, S., L. Xi, J. Ni, E. Pan, and C. R. Liu. 2008. "Product Lifecycle-oriented Quality and Productivity Improvement Based on Stream of Variation Methodology." *Computers in Industry* 59 (2–3): 180–192.
Du, S., J. Lv, and L. Xi. 2011. "Fault Diagnosis in Assembly Processes Based on Engineering-driven Rules and PSOSAEN Algorithm." *Computers & Industrial Engineering* 60: 77–88.
Du, S., J. Lv, and L. Xi. 2012a. "On-Line Classifying Process Mean Shifts in Multivariate Control Charts Based on Multiclass Support Vector Machines." *International Journal of Production Research* 50: 6288–6310.
Du, S., J. Lv, and L. Xi. 2012b. "A Robust Approach for Root Causes Identification in Machining Processes Using Hybrid Learning Algorithm and Engineering Knowledge." *Journal of Intelligent Manufacturing* 23: 1833–1847.
Du, S., D. Huang, and J. Lv. 2013. "Recognition of Concurrent Control Chart Patterns Using Wavelet Transform Decomposition and Multiclass Support Vector Machines." *Computers & Industrial Engineering* 66: 683–695.
Haller, M., A. Peikert, and J. Thoma. 2003. "Cycle Time Management During Production Ramp-up." *Robotics and Computer Integrated Manufacturing* 19: 183–188.
Hawkins, D. M. 1991. "Multivariate Quality Control Based on Regression-adjusted Variables." *Technometrics* 33 (1): 61–75.
Hawkins, D. 1993. "Regression Adjustment for Variables in Multivariate Quality Control." *Journal of Quality Technology* 25 (3): 170–182.
He, D., and A. Grigoryan. 2005. Multivariate Multiple Sampling Charts. *IIE Transactions* 37: 509–521.
Heredia-Langner, A., D. C. Montgomery, and W. M. Carlyle. 2002. "Solving a Multistage Partial Inspection Problem Using Genetic Algorithms." *International Journal of Production Research* 40 (8): 1923–1940.
Hu, M., Z. Lin, X. Lai, and J. Ni. 2001. "Simulation and Analysis of Assembly Processes Considering Compliant, Non-ideal Parts and Tooling Variations." *International Journal of Machine Tools and Manufacture* 41 (15): 2233–2243.
Huang, W., J. Lin, M. Bezdecny, Z. Kono, and D. Ceglarek. 2007a. "Stream-of-variation Modeling – Part I: A Generic Three-dimensional Variation Model for Rigid-body Assembly in Single Station Assembly Processes." *Journal of Manufacturing Science and Engineering* 129 (4): 821–831.
Huang, W., J. Lin, Z. Kong, and D. Ceglarek. 2007b. "Stream-of-variation (SOVA) Modeling – Part II: A Generic 3D Variation Model for Rigid Body Assembly in Multistation Assembly Processes." *Journal of Manufacturing Science and Engineering* 129 (4): 832–842.
Jiang, H. M., S. H. Li, H. Wu, and X. P. Chen. 2004. "Numerical Simulation and Experimental Verification in the Use of Tailor-welded Blanks in the Multi-stage Stamping Process." *Journal of Materials Processing Technology* 151 (1–3): 316–320.
Jin, J., and J. Shi. 1999. "State Space Modeling of Sheet Metal Assembly for Dimensional Control." *Journal of Manufacturing Science and Engineering* 121 (4): 756–762.
Jin, M., and F. Tsung. 2009. "A Chart Allocation Strategy for Multistage Processes." *IIE Transactions* 41: 790–803.
Koren, Y., U. Heisel, F. Jovane, T. Moriwaki, G. Pritschow, and G. Ulsoy. 1999. "Reconfigurable Manufacturing Systems." *CIRP Annals-Manufacturing Technology.* 48 (2): 527–540.
Loose, J. P., S. Zhou, and D. Ceglarek. 2007. "Kinematic Analysis of Dimensional Variation Propagation for Multistage Machining Processes with General Fixture Layouts." *IEEE Transactions on Automation Science and Engineering* 4 (2): 141–152.
Loose, J. P., Q. Zhou, S. Zhou, and D. Ceglarek. 2009. "Integrating Gd&T into Dimensional Variation Models for Multistage Machining Processes." *International Journal of Production Research* 48 (11): 3129–3149.
Mackertich, N. A. 1990. "Precontrol vs. Control Charting: A Critical Comparison." *Quality Engineering* 2 (3): 253–260.
Mardia, K. V., J. T. Kent, and J. M. Bibby. 1992. *Multivariate Analysis*. New York: Academic Press.
Niaki, S. T. A., and M. Davoodi. 2008. "Designing a Multivariate–Multistage Quality Control System Using Artificial Neural Networks." *International Journal of Production Research* 47 (1): 251–271.
Petersen, K. B., and M. S. Pedersen. 2006. *The Matrix Cookbook*. Kongens Lyngby: Technical University of Denmark.
Ramesh, R., M. A. Mannan, and A. N. Poo. 2000a. "Error Compensation in Machine Tools – A Review." *International Journal of Machine Tools and Manufacture* 40 (9): 1235–1256.
Ramesh, R., M. A. Mannan, and A. N. Poo. 2000b. "Error Compensation in Machine Tools – A Review." *International Journal of Machine Tools and Manufacture* 40 (9): 1257–1284.

Rowe, D. B. 2002. *Multivariate Bayesian Statistics*. New York: CRC Press.
Shamsuzzaman, M., Y. C. Lam, and Z. Wu. 2005. "Control Chart System with Independent Quality Characteristics." *The International Journal of Advanced Manufacturing Technology* 26: 1298–1305.
Shetwan, A. G., V. I. Vitanov, and B. Tjahjono. 2011. "Allocation of Quality Control Stations in Multistage Manufacturing Systems." *Computers & Industrial Engineering* 60 (4): 473–484.
Shi, J. 2006. *Stream of Variation Modeling and Analysis for Multistage Manufacturing Processes*. New York: CRC Press.
Shiau, Y. R. 2002. "Inspection Resource Assignment in a Multistage Manufacturing System with an Inspection Error Model." *International Journal of Production Research* 40 (8): 1787–1806.
Shin, Y. C., and Y. Wei. 1992. "A Statistical Analysis of Positional Errors of a Multiaxis Machine Tool." *Precision Engineering* 14 (3): 139–146.
Shu, L., F. Tsung, and K. C. Kapur. 2004. "Design of Multiple Cause-selecting Charts for Multistage Processes with Model Uncertainty." *Quality Engineering* 16 (3): 437–450.
Shu, L., F. Tsung, and K. L. Tsui. 2005. "Effects of Estimation Errors on Cause-selecting Charts." *IIE Transactions* 37 (6): 559–567.
Shi, J., and S. Zhou. 2009. "Quality Control and Improvement for Multistage Systems: A Survey." *IIE Transactions* 41 (9): 744–753.
Suri, R., K. Otto, and G. Boothroyd. 1999. "Variation Modeling for a Sheet Stretch Forming Manufacturing System." *CIRP Annals-Manufacturing Technology* 48 (1): 397–400.
Terwiesch, C., R. E. Bohn, and K. S. Chea. 2001. "International Product Transfer and Production Ramp-up: A Case Study from the Data Storage Industry." *R&D Management* 31 (4): 435–451.
Tsung, F., Y. Li, and M. Jin. 2008. "Statistical Process Control for Multistage Manufacturing and Service Operations: A Review and Some Extensions." *International Journal of Services Operations and Informatics* 3 (2): 191–204.
Veatch, M. H. 2000. "Inspection Strategies for Multistage Production Systems with Time-varying Quality." *International Journal of Production Research* 38 (4): 837–853.
Xiang, L., and F. Tsung. 2008. "Statistical Monitoring of Multi-stage Processes Based on Engineering Models." *IIE Transactions* 40 (10): 957–970.
Xie, K., L. Wells, J. A. Camelio, and B. D. Youn. 2007. "Variation Propagation Analysis on Compliant Assemblies Considering Contact Interaction." *Journal of Manufacturing Science and Engineering* 129 (5): 934–942.
Zhang, S., and Z. Wu. 2006. "Monitoring the Process Mean and Variance Using a Weighted Loss Function CUSUM Scheme with Variable Sampling Intervals." *IIE Transactions* 38: 377–387.
Zhou, S., Q. Huang, and J. Shi. 2003. "State Space Modeling of Dimensional Variation Propagation in Multistage Machining Process Using Differential Motion Vectors." *IEEE Transactions on Robotics and Automation* 19 (2): 296–309.
Zou, C., F. Tsung, and Y. Liu. 2008. "A Change Point Approach for Phase I Analysis in Multistage Processes." *Technometrics* 50 (3): 344–356.

Appendix 1. The HTM matrix

Denote the characteristic N's location in the RCS is H_N^R.

$$H_N^R = \begin{bmatrix} \mathbf{R}_N^R & \mathbf{t}_N^R \\ \mathbf{0} & 1 \end{bmatrix}$$

where $\mathbf{R}_N^R$ is the rotational sub-matrix and $\mathbf{t}_N^R$ is the positional vector. $\mathbf{R}_N^R$ represents the rotational movement from one coordinate system to another and $\mathbf{t}_N^R$ represents the positional movement from coordinate system to another. Figure A.1 shows that the transformation of the coordinate system from $O_0X_0Y_0Z_0$ to $O_1X_1Y_1Z_1$ contains a positional operation $\mathbf{T}$, and the rotational operation $[\alpha, \beta, \gamma]$. And the corresponding HTM is $H_0^1 = \begin{bmatrix} \mathbf{R}_{\alpha\beta\gamma} & \mathbf{T} \\ \mathbf{0} & 1 \end{bmatrix}$.

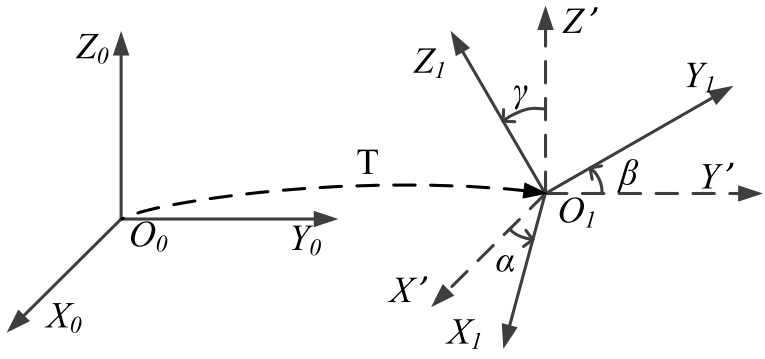

Figure A.1. Homogenous transformation.

Appendix 2. The state-space model for the turning process

The state-space model of the turning process is illustrated as follows. Take the conventional 4-jaw chuck fixture scheme for example (see Figure 2(a)). When clasped tightly in the 4-jaw chuck, the part's 6 degrees of freedom can be imagined as fixed. Then, locators can be abstracted form the original fixture (see Figure A.2(b)).

The locator L3 is presented for the equivalent locator when the clamp force is enough to limit the rotational movement with respect to Y_F. Under such locator assumption, the datum induced error can be figured out. The datum error is the variation between the RCS and the FCS. And the total datum error can be expressed by the combination of the primary datum plane (denoted as characteristic 1) variation with respect to RCS, and the variation of the secondary datum and the tertiary plane (denoted as characteristic 2, 3) with respect to RCS. Thus, the datum induced error can be (A.1)

$$x_{\mathrm{FCS}(k)}^{R(k)} = T_1(k)x_{r_1(k)}^{R(k)} + T_2(k)x_{r_2(k)}^{R(k)} + T_3(k)x_{r_3(k)}^{R(k)} \tag{A.1}$$

The following equation system (A.2) holds because this engagement means the Z coordinate in the corresponding LCS for certain locators' ending is zero.

$$\begin{cases} [H_R^1 \cdot H_F^R \cdot \tilde{p}_1^F]_3 = 0 \\ [H_R^1 \cdot H_F^R \cdot \tilde{p}_2^F]_3 = 0 \\ [H_R^1 \cdot H_F^R \cdot \tilde{p}_3^F]_3 = 0 \\ [H_R^2 \cdot H_F^R \cdot \tilde{p}_4^F]_3 = 0 \\ [H_R^2 \cdot H_F^R \cdot \tilde{p}_5^F]_3 = 0 \\ [H_R^3 \cdot H_F^R \cdot \tilde{p}_6^F]_3 = 0 \end{cases} \tag{A.2}$$

where $\tilde{p}_i^F$ is the adjusted vector, $\tilde{p}_i^F = \left[\left(p_i^F\right)^T \quad 1\right]^T$, and H_F^R is the HTM from the FCS to RCS, and H_R^i is the HTM from RCS to LCS$_i$. Since p_i^F and the nominal HTM ${}^0H_F^1 \sim {}^0H_F^3$ can be measured directly, the six non-zero element matrix H_F^R, therefore, can be solved in (A.2). By rearranging the answer in (A.1) form, the coefficient matrix of datum error $A_2(k)$is (A.3).

$$A_2(k) = [0 \cdots T_1(k) \cdots T_2(k) \cdots T_3(k) \cdots 0]_{6\times 6M} \tag{A.3}$$

The fixture error can be deduced by applying the result of (Cai, Hu, and Yuan 1997). And the coefficient matrix of datum error is (A.4), where L is the depth of the part been clasped.

$$A_3 = \begin{bmatrix} 0 & 0 & 0 & -1 & 0 & 0 \\ \frac{-L_{6x}}{L} & \frac{L_{6x}}{L} & 0 & \frac{L_{6z}}{L} & \frac{-L_{6z}}{L} & -1 \\ -1 & 0 & 0 & 0 & 0 & 0 \\ \frac{-1}{L} & \frac{1}{L} & 0 & 0 & 0 & 0 \\ \frac{L-L_{3y}}{L\cdot L_{3z}} & \frac{L_{3y}}{L\cdot L_{3z}} & \frac{-1}{L_{3z}} & 0 & 0 & 0 \\ 0 & 0 & 0 & \frac{1}{L} & \frac{-1}{L} & 0 \end{bmatrix} \tag{A.4}$$

A_1 and A_4 are transforming matrix, which can be gotten through HTM. And A_5 is the selective matrix, with the identity elements corresponding to the indexes of the characteristics manufactured at kth stage.

Appendix 3. Simulation case

The simulation study is based on X-armature, whose shape is illustrated by Figure A.3. The corresponding clamping scheme in each step of the manufacturing process is illustrated by Figure A.4. Variation transmission effect between stages is shown in Figure A.4

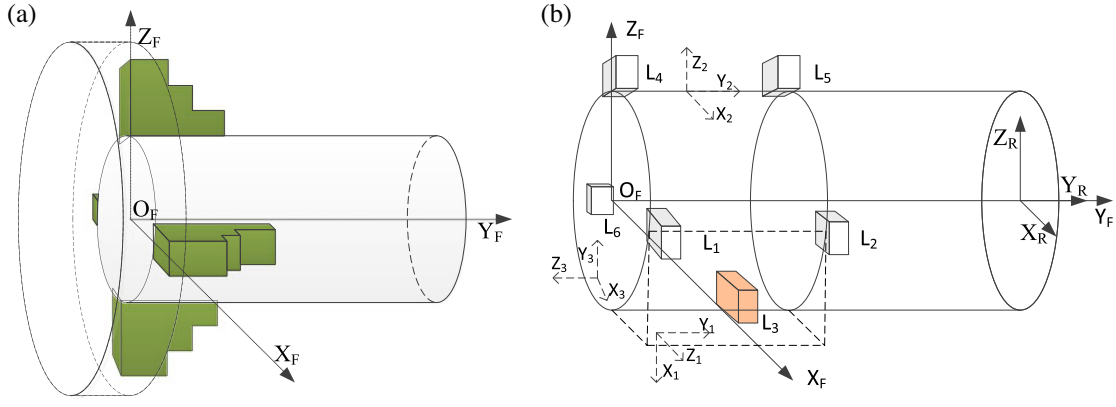

Figure A.2. Locator analysis of turning process. (a) fixture scheme and (b) locators illustration.

evidently. To illustrate the proposed method and keep the scope of this paper, we simply study the dimensional error of the excircle of X-armature, omitting other interior features.

The engineering model is constructed according to the procedure depicted in Figure 4. In this case, the fixture error of each stage is fixed once generated from a multivariate normal distribution, while the tool errors are changing in each time and the tool errors follow a multivariate normal distribution. This error generating scheme is built to simulate the error generation in real world manufacturing process. These generated errors are inserted into the model to depict the stream of variation in MMPs and the proposed method.

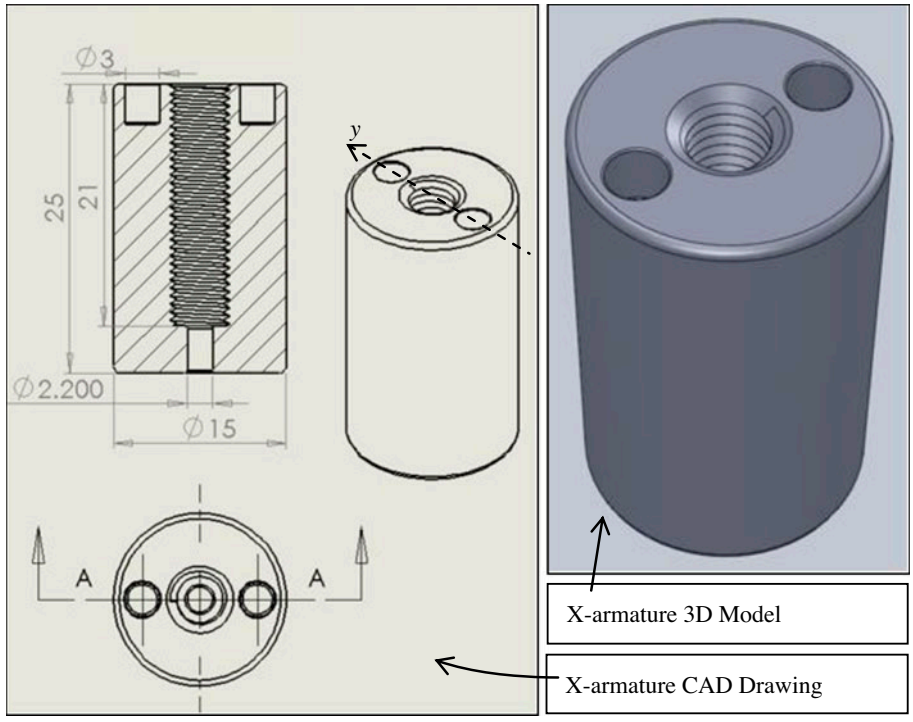

Figure A.3. X-armature model.

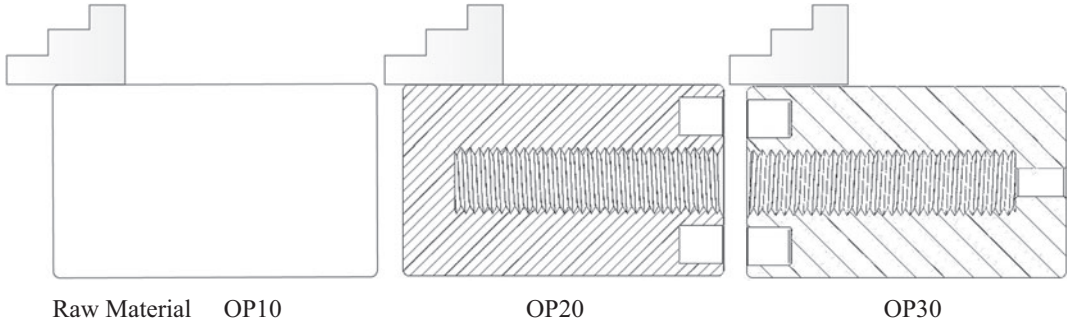

Figure A.4. Manufacturing process illustration.